Micro-hydroelectric Intake and Greenhouse Design

A Major Qualifying Project
Submitted to the Faculty of the
Worcester Polytechnic Institute
In partial fulfillment of the requirements for the
Degree of Bachelor of Science

Submitted on: April 25, 2017

By:
Aaron McGinnis (CHE)
M. Paige Myatt (ME)
Nathan Peterson (ME)

For: Te Runanga o Ngāti Kea Ngāti Tuara of Horohoro, New Zealand

NGĀTI KEA NGĀTI TUARA

Approved By:
Advisor: Professor Robert Daniello (ME)
Co-Advisor: Professor Stephen Kmiotek (CHE)

Abstract

The purpose of this project was twofold: a) to mitigate intake congestion of a micro-hydro power system at the Kearoa Marae in Horohoro, New Zealand, and b) to develop a basic feasibility assessment focusing on resource requirements for a commercial scale hydroponic greenhouse that would utilize electricity generated by the hydroelectric unit. To address the congestion of the micro-hydro intake, our team designed, constructed, and installed a self-cleaning floating boom across the inlet of the system to deter floating debris from entering the inlet, as well as a mesh screen to catch any submerged debris, reducing maintenance time and allowing the system to produce electricity to its fullest potential. Modeling the hydroponic greenhouse resulted in estimated heating, water, and electricity requirements that were used to develop recommendations to our sponsor, Te Runanga o Ngāti Kea Ngāti Tuara.

Acknowledgements

Our MQP group extends a special thanks to our project advisors Professor Robert Daniello and Professor Stephen Kmiotek for their excellent advising during our work in New Zealand and our time at WPI. We would also like to recognize Professor Ingrid Shockey and Professor Dominic Goulding for providing local support while we were in New Zealand. This project would not have been possible without the support of our sponsor Ngāti Kea Ngāti Tuara. Specifically, we would like to thank Eugene Berryman-Kemp for serving as our main liaison, Riki Oneroa for his support and guidance on-site, and Kataraina George for her assistance. For their help with hydroponic greenhouse design, we would like to thank Neville Stocker of PGO Horticulture LTD and Paul Mes of Pure Hydroponics. We would also like to thank Alden Hydraulic Research Laboratory in Holden, MA for giving us a tour of their facilities and sharing their knowledge on hydroelectric intake models. Additionally, we extend our gratitude to the WPI Department of Mechanical Engineering and the WPI Department of Chemical Engineering for their support. Lastly, we thank Professor Mike Elmes and the WPI Global Studies Division for helping bring this project to fruition and ensuring a safe trip abroad.

Table of Contents

List of Figures

List of Tables

Chapter 1: Introduction

The rural area of Horohoro, New Zealand is home to the indigenous Māori community of Ngāti Kea Ngāti Tuara (NKNT). The center of this community is the Kearoa Marae, a spiritually significant meeting house in which members come together to celebrate important life events. The Pokaitu stream runs behind the marae, through several farms that surround the area and paint the pastoral scenery. As a part of NKNT's commitment to preserving the environment and practicing sustainability, a series of three micro-hydroelectric turbines were installed in December 2013 to power the marae and surrounding farm. Since this installation, the unit has consistently output 2.3-2.5 kW of electricity, which is more than the buildings it powers currently consume. In many months, less than half of this energy is used by the community, and the rest is sold back to suppliers at a third of the purchase price from the electric grid. To satisfy their economic, environmental and community goals, NKNT aspires to use this available electricity to power a hydroponic greenhouse.

The micro-hydro unit requires regular maintenance, primarily by Mr. Riki Oneroa, for its continual, efficient operation. Before our team's project took place, Riki had to clear leaves, sticks and other debris daily from the intake grate that protects the system from such obstructions. This task required Riki to use either his hands or a rake to clean the grating, which is neither enjoyable nor ergonomic.

Our team was thus presented with two tasks: mitigate the micro-hydro unit's debris congestion, and model a hydroponic greenhouse to estimate heating, equipment and water requirements to determine its feasibility. After research and discussions with NKNT, we decided to pursue the design, construction, and implementation of a floating boom and mesh system that would direct floating debris downstream and away from the intake and catch submersed objects. This solution would reduce the time it takes Riki to maintain the system and improve its efficiency. Additionally, we investigated the feasibility of constructing a hydroponic greenhouse in the community that would run primarily on electricity from the turbine unit. The greenhouse system would provide a means of capitalizing on excess energy production in a manner consistent with NKNT's values regarding sustainability and the environment. Additionally, it has the potential to provide jobs to community members and become a source of revenue for NKNT.

Chapter 2: Background

This chapter puts the scope of the project into perspective by providing background information on pertinent Māori culture, the community of Ngāti Kea Ngāti Tuara (NKNT), their micro-hydro power system and its intake congestion problem, along with NKNT's considerations regarding the design and construction of a greenhouse.

2.1 Brief History of New Zealand

The Māori are the indigenous population of Aotearoa / New Zealand, traveling to the island country in *waka* (canoes) from other islands in the South Pacific over 1000 years ago. The Europeans first discovered New Zealand in 1642, but did not make landfall until 1769 when Captain James Cook and other Englishmen began to settle the islands. In an attempt to gain control of the land and come to a mutual understanding of its ownership and use, New Zealand's first governor, William Hobson, and Māori chiefs from across the country came together to sign The Treaty of Waitangi in 1840.

The treaty came with great misunderstanding. The Māori had gifted the land to the Europeans to protect it as guardians. The Europeans did not see it this way and viewed the land as theirs to use however they pleased. The misinterpretation of the treaty led to war in which more of the Māori's land was lost to the creation of expansive farms and developing townships ("A Brief History", 2016). In 1975, the New Zealand Government, in cooperation with the Māori, formed the Waitangi Tribunal, which was set up to settle land claims in an attempt to return some of the land to the Māori. Unfortunately, most of the land will likely never be returned and settling these land claims is a lengthy and complex process, but it is a step in the right direction ("Waitangi Tribunal", 2016).

2.2 Ngāti Kea Ngāti Tuara

Horohoro is home to the Māori community of Ngāti Kea Ngāti Tuara. It is a rural town located 16 kilometers southwest of Rotorua and part of the greater Bay of Plenty Region, as shown on the map in Figure 1. The NKNT tribe, or *iwi*, consists of approximately 1,500 members over the age of 18: 60% live in the Bay of Plenty region, 30% live in other parts of New Zealand, and 10% live overseas. Very few actually live in Horohoro (Bargh, 2015). A *hapū* is a smaller grouping within the iwi. Iwi member and NKNT Project Manager, Eugene Berryman-Kamp, served as this project's sponsor and primary contact person for the students.

Figure 1: Map of New Zealand's North Island with major cities and outlined Bay of Plenty Region

2.2.1 Land Settlements

The ancestral lands of Ngāti Kea Ngāti Tuara once covered 50,000 acres around Horohoro. Today there are only about 4,000 acres of land left in hapū guardianship. Over 60% of that is for farm land and forestry. NKNT has set aside the remaining as land reserve. Ngāti Kea Ngāti Tuara, as an affiliate of Te Pumautanga o Te Arawa (a post-settlement governance entity), is working to regain some of their traditional lands as part of a Treaty of Waitangi settlement. ("History | Ngāti Kea Ngāti Tuara", 2016).

2.2.3 Values

The Māori have a deep connection with their values and traditions. Three of their values that have the greatest influence on this project are whakapapa, kaitiakitanga, and no te hapū. Whakapapa translates to genealogy and is important when considering land and its relationship to people. Like humans and animals, the land and water have their own whakapapa and ancestry (Bargh, 2012). Perhaps the Māori's deepest connection is with the land, as they call themselves "tangata whenua" or "people of the land". Closely related to this connection with the land comes the value Kaitiakitanga, which implies environmental guardianship. The Māori have strong ties to the Earth and are thus extremely environmentally aware (Royal, 2007). A third value important for the team to consider is "no te hapū", which indicates a strong desire for communal benefit over the benefit of an individual (Bargh, 2012). Any project must take into consideration its societal impacts on the community. Ngāti Kea Ngāti Tuara has outlined goals for any community project to reflect these core Māori values. Every undertaking must satisfy their 4-fold bottom line that addresses economic, environmental, social, and cultural standards (Berryman-Kamp, 2016). These are all equally important values to consider, and the team must account for any impact the project may have on these standards.

2.2.4 Project History

In December 2013, Ngāti Kea Ngāti Tuara installed a micro-hydro unit consisting of three hydroelectric turbines that generate electricity from a waterfall on the Pokaitu Stream, which flows directly behind the hapū's *marae* (meeting house). To do so, Te Runanga o Ngāti Kea Ngāti Tuara, the governing council of the hapū, worked in conjunction with EcoInnovation Ltd of New Zealand, the designer and manufacturer of the PowerSpout equipment used in the unit. With this system, they produce enough electricity to power their community buildings and iwi-owned farm. NKNT's micro-hydro project has been in the

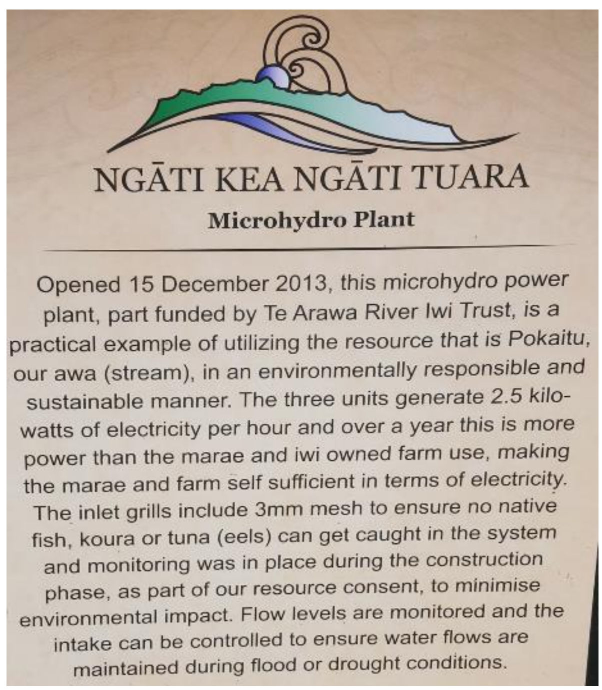

Figure 2: Sign with the micro-hydro system's history at NKNT

news, setting a great example for other Māori communities (see Appendix 6.1 News Articles and Publicity of Micro-hydro Project).

Hydropower and other sources of renewable energy, such as geothermal, are common throughout New Zealand. NKNT's project exemplifies one of the many ways other iwi can continue their commitment to sustainability by using the renewable resources they have around them. However, the NKNT's system currently suffers from an intake congestion problem. Small debris, such as pine needles and other foliage, from the Pokaitu stream, a tributary of the Waikato River, clog the intake. Iwi member and property maintenance manager, Riki Oneroa, is the primary caretaker of the turbines. In working closely with the turbines for the past three years, he has become an expert on the system. With debris-filled water freely flowing into the inlet, he must clean the intake grate on a daily basis. This Major Qualifying Project (MQP) focuses directly on this aspect of the micro-hydro system and aims to design and implement an eco-friendly solution that will alleviate the intake congestion and need for daily cleaning.

The Interactive Qualifying Project (IQP), "Assessing Greenhouse Feasibility: A Report to the Ngāti Kea Ngāti Tuara Hapū of Horohoro, New Zealand", completed by two returning team members, Nathan Peterson and Paige Myatt, in 2016, served as the basis for this Mechanical Engineering and Chemical Engineering MQP and briefly addressed the need for a solution to this intake congestion problem. The IQP's main focus was to produce a feasibility report regarding the perception of a greenhouse in the community that would be powered by the micro-hydro system.

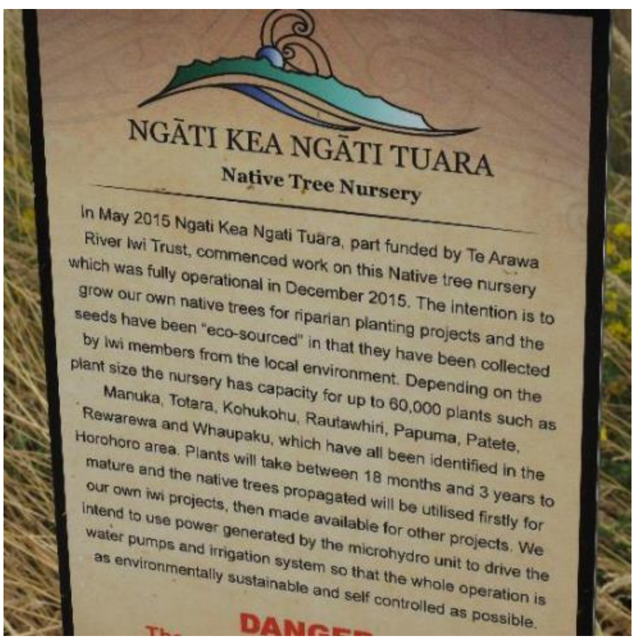

Figure 3: Native Tree Nursey Sign at NKNT

The project examined possible crops to grow in addition to identifying potential business opportunities. From their research the team learned that the greenhouse would initially be best suited for community use and development. Since then, NKNT has pursued the idea of a greenhouse and is currently constructing a small structure in which to grow native trees to be utilized in riparian planting, seen in Figure 4. The community is in the process of planting these trees on the banks of the Pokaitu Stream as part of a river clean-up project; their purpose is to absorb the farm runoff and prevent it from entering the water, described in Figure 3.

Figure 4: Greenhouse set up for construction with native plants

2.3 Micro-hydro System Overview

This section is most easily explained with a visual representation. Figure 5 shows a simplified diagram of a micro-hydro system overlaid by photographs of NKNT's setup.

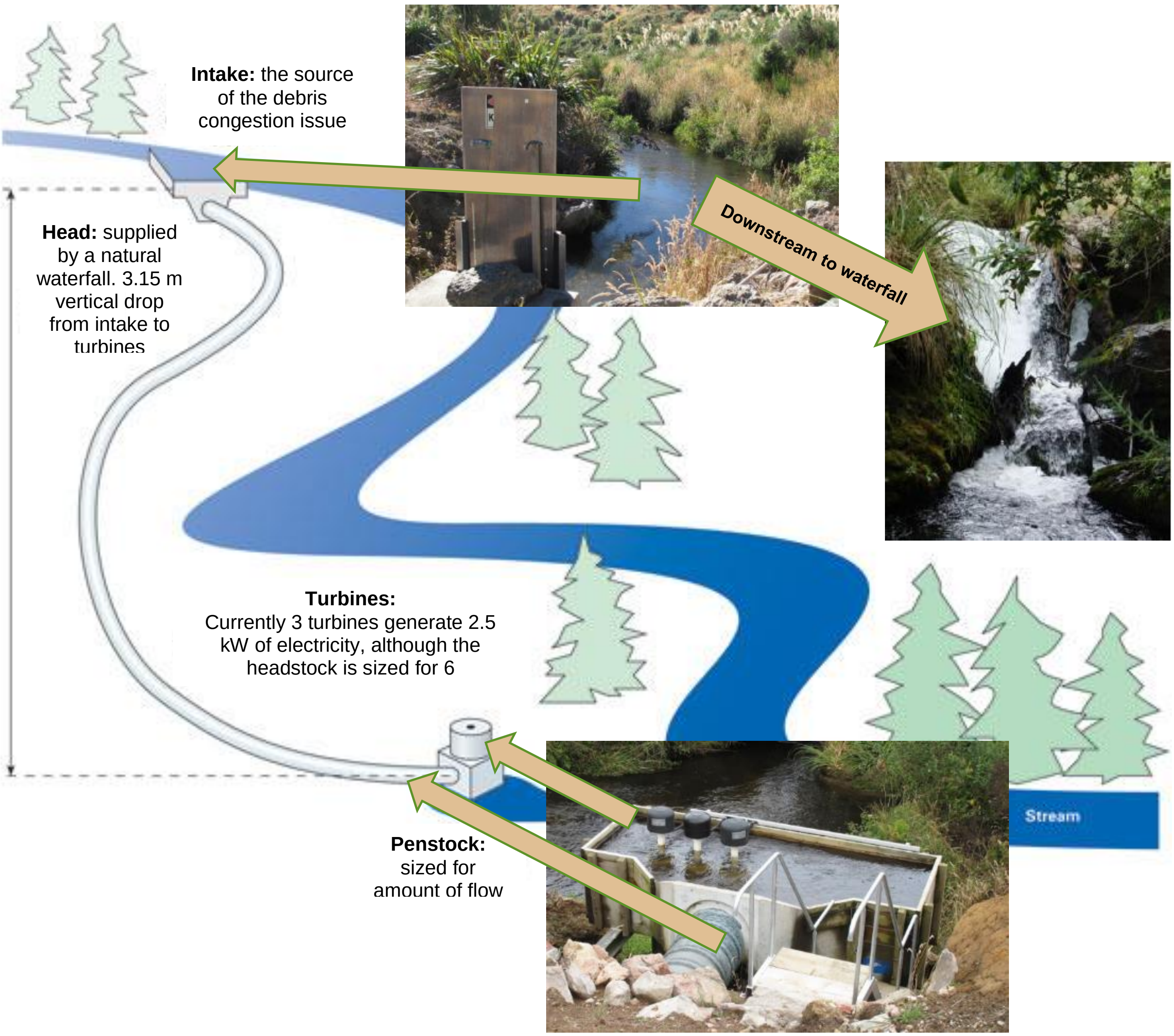

Figure 5: NKNT's micro-hydro set up, pre-boom installation

2.3.1 The Pokaitu Stream

The Pokaitu Stream is relatively narrow and slow-moving as it passes Ngāti Kea Ngāti Tuara. Data taken by the Waikatu Regional Council just 3 kilometers downstream indicates that summer flows range from 700 – 1600 liters per second (L/s). With each turbine requiring 50 L/s, and a minimum required flow rate with 6 turbines of 300 L/s, the stream offers enough flow for optimal operation. Table 1 displays data from the PowerSpout Case Study gathered by the National Institute of Water and Atmosphere Research, Ltd (NIWA). Flooding is not uncommon in the stream and can be harmful to the micro-hydro unit if the appropriate precautionary measures are not taken. In the event of a flood, a community member, mainly Riki, must block off the intake by dropping a large metal door that stops water from entering the penstock, as seen in Figure 6.

Catchment Area	31.9 km^2
Mean Annual Rainfall	1640 mm
Mean Flow	897 L/s
Annual Flood Flow	8.7 m^3/s
100-year Flood	23.9 m^3/s

Table 1: Pokaitu Steam Data (PowerSpout, 2014)

Figure 6: Micro-hydro Intake

The design of the unit at NKNT utilizes a drop in head resulting from a small waterfall in the stream 3.15 meters in height. The intake is upstream of the waterfall, feeding water through the supply pipe to the headstock downstream. Figure 7 shows an aerial view of the area.

Figure 7: Aerial view of the stream and intake

2.3.2 Headstock Design

Steel girders set in concrete and pilings bedded in the riverbank support the headstock. The top of the concrete trough lies below the intake level and allows water expended by the turbines or any excess water to return to the river below. Figure 8 shows the headstock without turbines and the waterfall behind it.

Figure 8: Headstock and waterfall (PowerSpout, 2014)

2.3.3 Power Generation

The turbines employed in the design are PowerSpout LH (low head) turbines, each capable of producing 700-800 Watts and requiring a flow rate between 25 and 55 L/s and 1-5 meters of head. EcoInnovation designed the headstock to fit 6 turbines, but only 3 turbines are currently installed and the remaining three holes are sealed. Still, the system generates up to 2.5 kW, which exceeds the amount of energy typically consumed by the marae and surrounding buildings. Figure 9 displays Riki with one of the three turbines.

Figure 9: Riki with the turbines

2.3.4 Intake Design

EcoInnovation constructed the intake of the system from a concrete septic tank measuring 2.21 meters in length with two holes on each end for water flow and one hole on top for accessibility and maintenance. Figure 12 shows the bare tank in the trench during construction.

Figure 10: Intake (2017)

The supply pipe that enters the tank is 600 mm in diameter. Figure 11 shows the pipe within the tank, perforated with holes 50 mm in diameter. Large rocks surround the intake to minimize erosion. The entrance to the tank features a flow control mechanism in which a metal gate slides along a track to partially or completely cover the entrance, allowing flow to be diminished or completely cut off in flood conditions, as previously mentioned. The grill at the entrance stops larger debris from going inside the tank. Figure 10 shows a side view of the intake.

Figure 11: Perforated pipe (PowerSpout, 2014)

Figure 12: Septic tank intake (PowerSpout, 2014)

2.3.5 Problem Definition

The micro-hydro unit has been successful in generating power for Ngāti Kea Ngāti Tuara, but intake congestion problems caused by debris diminish or halt the output of the turbines until cleaned. To mitigate this problem, Riki installed a temporary debris catching device made out of windscreen mesh, which is typically used on fences, fastened to a gate wedged in the inlet to block debris across the entrance of the intake. Figure 13 shows the inlet to the intake and this temporary screen. However, this structure has since been washed away in a large storm, leaving the intake protected only by a wide grill, as seen previously in Figure 6. This intake grill is not sufficient for blocking smaller debris, and allows small leaves, algae, and other foliage to enter the system. The initial design included a 3 mm metal mesh screen, shown in Figure 14 that is inserted beyond the wider grate and covers the perforated supply pipe within the tank. With no other inlet protection, debris clogs this mesh within a few hours and must be cleaned before the turbines can continue to generate electricity. Therefore, it remains unused and is laid on the rocks of the intake, as seen in Figure 13.


Figure 13: Intake with mesh gate (2016)

Although the temporary screen helped to keep the smaller debris clear of the intake, it frequently became blocked and thus restricted flow to the micro-hydro. The screen had to be manually cleared as often as daily, depending on the season. Figure 15 shows the screen blocked with debris, thus limiting the flow able to pass through it.


Figure 14: Unused metal mesh screen


Figure 15: Close-up of previous intake debris solution (2016)

The team’s primary goal is to design and implement an eco-friendly mechanism that will deflect debris downstream and thus prevent it from entering the intake of the micro-hydro unit while not restricting flow. In doing so, we will assist Ngāti Kea Ngāti Tuara in producing energy to the full potential of their micro-hydro.

2.4 Greenhouse Project Overview

Farming and forestry consumes 2,500 acres of the land left in hapū guardianship. Several environmental challenges result from this widespread farming, including stream bank sediment erosion from riparian zone clearing and waterway pollution resulting from fertilizer runoff. To help prevent soil erosion and fertilizer runoff from entering freshwater resources, NKNT has planted native trees alongside riverbanks to assist in cleanup and runoff prevention, a practice known as riparian management (George, 2016). Many of these trees were grown in a small greenhouse owned by NKNT community member, Bob Young, which is located up the road from the Kearoa Marae. Once the trees have developed enough to survive outside, they are potted and maintained on a small plot of land near the micro-hydro unit as shown in Figure 16. Riki and Eugene oversee this operation. In the summer, up to three student interns assist Riki with the project.

Figure 16: Potted native trees (2017)

In August of 2016, NKNT put in an application to the Waikato Regional Council to receive funding for a $500,000, 5-year greenhouse project that would grow 40,000 native trees for riparian planting on a 6 m X 16 m plot highlighted as two separate areas in Figure 17. The Waikato River Authority, the entity responsible for restoration and protection initiatives of the river, refused this funding request ("Purpose", 2016). Upon further consideration, NKNT has chosen to keep the riparian tree nursery relatively small scale, growing 5,000 plants a year. Instead, they are interested in pursuing a large-scale, hydroponic greenhouse in the coming years.

Figure 17: Initial map of greenhouse plan (NKNT, 2016)

According to Eugene, construction of a hydroponic greenhouse would likely take place 3-5 years in the future, so our team decided to focus on an initial greenhouse feasibility assessment emphasizing technical design aspects. Specifically, we have estimated the amount of heating, water, and electricity required to operate a greenhouse of the same dimensions as proposed riparian tree nursery expansion project. We have also included a cost estimate. With these key parameters identified, our sponsor has useful information to begin the application and decision-making process for this project. Additionally, we have laid the groundwork for additional design work to be completed and have provided contacts for potential suppliers of hydroponic and greenhouse equipment. If the board decides to approve the completed application, a hydroponic greenhouse could be constructed in the next 3-5 years, providing a source of revenue for the trust, creating 2-3 jobs for local residents, and effectively utilizing electricity produced by the micro-hydro unit.

Chapter 3: Methodology

The team took three trips to the project site in Horohoro, each of which lasted four to five days. The timeline of the team's seven working weeks spent in New Zealand, location and description of project work follows in Table 2:

Time	Location	Activity
Week 1 (January 16-20, 2017)	Horohoro	Site assessment
Week 2 (January 23-27, 2017)	Wellington	Boom design calculations
Week 3 (January 30 - February 3, 2017)	Wellington	Sourcing boom materials
Week 4 (February 7 - 10, 2017)	Horohoro	Boom construction and installation
Week 5 (February 13 - 17, 2017)	Wellington	Greenhouse design modeling
Week 6 (February 20-23, 2017)	Horohoro	Boom refinement and mesh addition
Week 7 (February 27 - March 3, 2017)	Wellington	Report writing and continued greenhouse modeling
Post-project trip (March 16-17, 2017)	Horohoro	Post-storm assessment and adjustment

Table 2: Project Timeline

The initial trip to Horohoro took place during the first of seven weeks, almost immediately after our arrival in New Zealand. We spent the following two weeks in Wellington, where we developed the design for the boom and ordered materials remotely in anticipation of our second trip to the project site. During the second trip, the team picked up materials in nearby Rotorua, constructed the floating boom according to the final design, and installed it across the micro-hydro inlet by anchoring to the surrounding banks of the Pokaitu stream. With the floating boom functioning as planned, and needing only minor refinements before our final trip to the project site, week five was dedicated largely to the modeling and assessment of the feasibility of a commercial hydroponic greenhouse at the site. The final trip to Ngāti Kea Ngāti Tuara allowed us to make modifications to the boom design. The team also installed a mesh screen parallel to but independently of the boom during this final trip. The final week in New Zealand was spent in

Wellington, finalizing the modeling and estimation of annual energy and water usages and cost. Team member Paige was able to make a post-project trip up to the site two weeks after the team's final visit. This trip was well-timed, as a 20-year storm had just passed through the area in the previous week, flooding the stream and causing some damage to the boom. Paige was able to make some final adjustments and correct the issues with the boom.

3.1 Preliminary Research

3.1.1 Micro-hydro Intake Literature Review

In Serious Micro-hydro: Water Power Solutions from the Experts, Jerry Ostermeier details intake designs and slow-water zone diversions, one of which employs a floating boom to deter debris, shown in Figure 18.

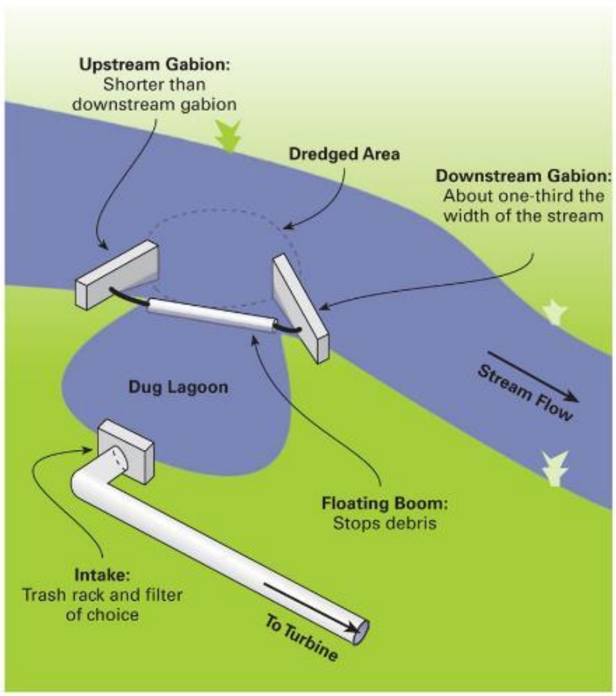

Figure 18: Possible Intake Design (Ostermeier, 2008)

This design also employs gabions and a dredged area. Due to the restrictions surrounding resource consent and the short time frame of our visit, the team could not make any permanent, large-scale adjustments to the intake to include such features.

Elastec, a company based in the United States, manufactures a "Floating Net Boom Barrier", albeit on a much larger scale than our project, but its design and materials may be of use to consult as we address this problem (Figure 19).

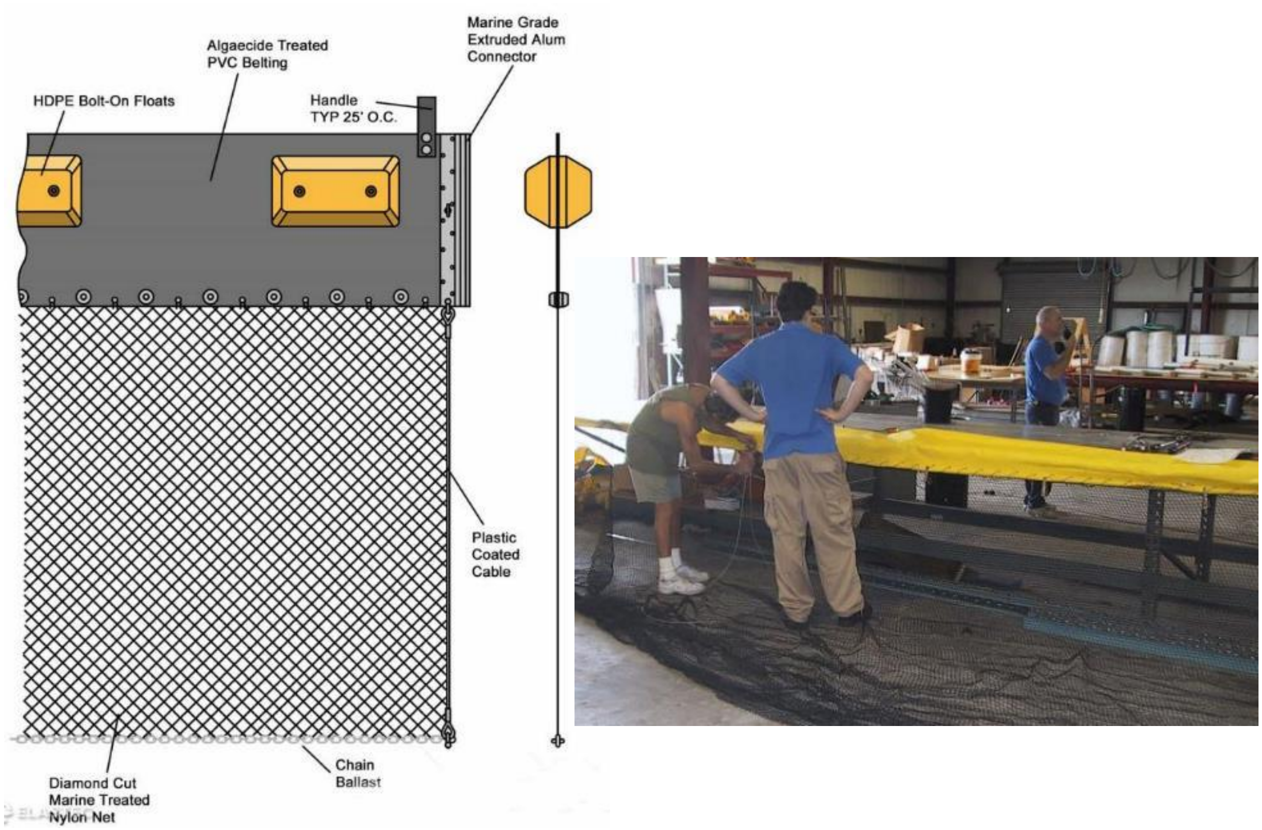

Figure 19: Elastec floating net boom ("Floating Marine Trash and Debris | Containment Boom | Elastec", n.d.)

Because the intake design of NKNT's micro-hydro cannot reasonably be altered, our team intends to investigate the potential for the implementation of a floating boom that eases or resolves the habitual intake congestion of the micro-hydro and can withstand and adapt to changing river conditions. We will determine and account for all significant design, material, construction, and installation considerations in order to meet these ends.

3.1.2 Alden Lab Visit

On November 30, 2016, team members Nathan and Paige took a trip with project advisor Professor Robert Daniello to Alden Lab in Holden, MA. This fluids laboratory works on solving a variety of flow problems through physical modeling. Many of these problems are applicable to our project. In the tour around the facility, employees of the lab showed us models they are working on regarding hydropower systems and intake debris congestion. A model of a floating boom design used at the Clifty Creek Power Plant in Madison, Indiana was the most applicable possible solution to NKNT's intake congestion. Figure 20 shows the model of the boom and a hand drawn sketch.

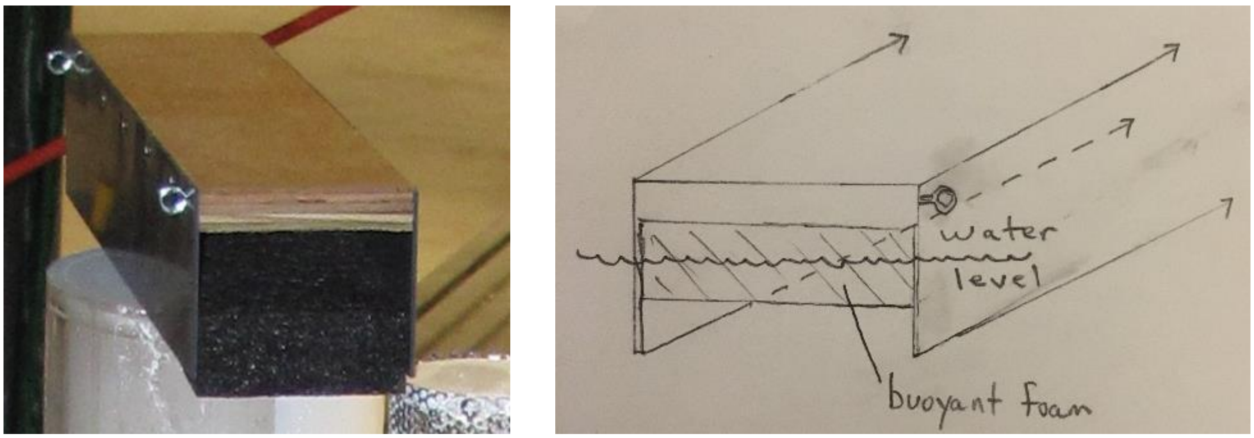

Figure 20: Clifty Creek Power Plant Floating Boom Model at Alden Lab (2016)

Upon further research, the team discovered the full-scale floating boom in action on Google Maps, as seen in Figure 21. This basic concept served as the basis for the team's proposed solution.

Figure 21: Aerial view of full-scale floating boom in action at Clifty Creek Power Plant (Google Maps, 2017)

3.1.3 Greenhouse Literature Review

Hydroponics

While traditional greenhouses grow plants in soil, hydroponics involves growing plants in soilless media containing a nutrient rich solution ("Hydroponic Systems 101," n.d.). Globally, hydroponic greenhouse systems cover approximately 20,000 to 25,000 hectares of land, producing over 6 billion dollars in revenue form produce ("Hydroponics," 2015). Hydroponic systems allow for tight control of nutrients contributing to plant growth, resulting in healthier produce and higher yields ("What is hydroponics?" 2008). Plant roots are at all times in contact with nutrients in specific concentrations that are suited for optimum growth, and nutrient concentrations can be easily adjusted as well as the pH. According to Full Bloom Hydroponics, hydroponic plants grow 25 percent faster than traditionally grown crops and yields are 30 percent higher ("Hydroponic Systems 101," n.d.). The main disadvantages of hydroponic systems are high cost and high maintenance, relative to soil-based systems.

Six different types of hydroponic systems dominate this market. Figure 22 summarizes these techniques.

1. Deep Water Culture (DWC)
2. Nutrient Film Technique (NFT)
3. Aeroponics
4. Wicking
5. Ebb & Flow
6. The Drip System

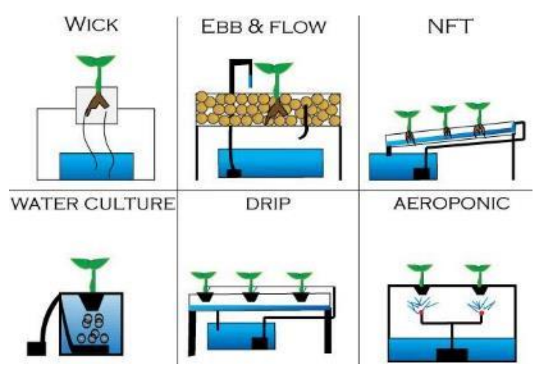

Figure 22: Summary of six hydroponic growing techniques ("Nutrient Film Technique," 2017.)

DWC, shown in Figure 23, involves growing plants in a reservoir filled with the appropriate nutrient solution. In this technique, roots are always suspended in the nutrient solution. An air pump is used to oxygenate the nutrient solution to promote nutrient uptake, thus avoiding

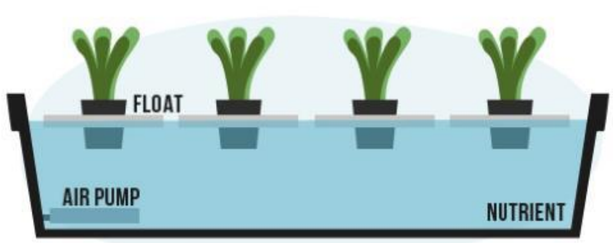

Figure 23: Deep Water Culture Diagram ("Deep Water Culture," n.d.)

plant starvation. DWC systems are relatively simple from a technical standpoint, and they are also inexpensive.

In contrast to DWC, NFT systems, explained in Figure 24, incorporate continuous flow of a nutrient solution over plant roots rather than bubbling water. They are built with an intentional slope that allows water to be gravity fed back into the solution tank. An air pump is typically not required for this system because the nutrient solution contacts only the base of the roots, leaving the remainder exposed to the air ("Hydroponic Systems 101," n.d.). The main drawback of NFT systems are sensitivity to water flow interruptions, which can cause plants to wilt quickly since nutrients are not stored in the growth medium ("N.F.T. System," n.d.). This system is highly resource efficient as a result of the recirculation system ("Commercial hydroponic," 2017).

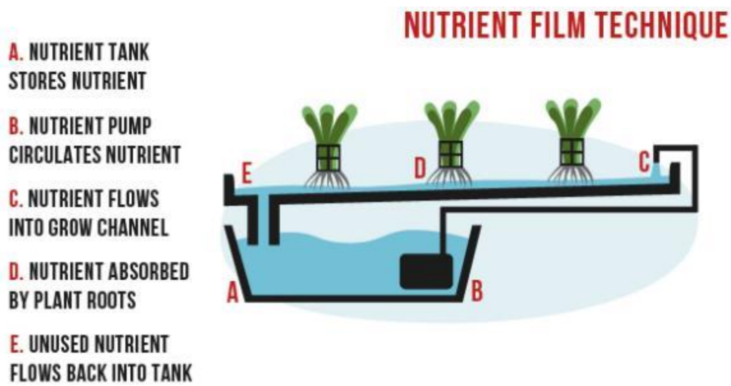

Figure 24: Nutrient film technique (Gurtler, 2014)

While DWC and NFT systems utilize a layer of nutrient solution having a specified depth, aeroponic systems, as seen in Figure 25, mist the solution onto roots directly ("Our Technology," n.d.). Supplier AeroFarms claims that aeroponic systems use "95% less water than field farming, 40% less than hydroponics, and zero pesticides." Similar to NFT systems, plants grown

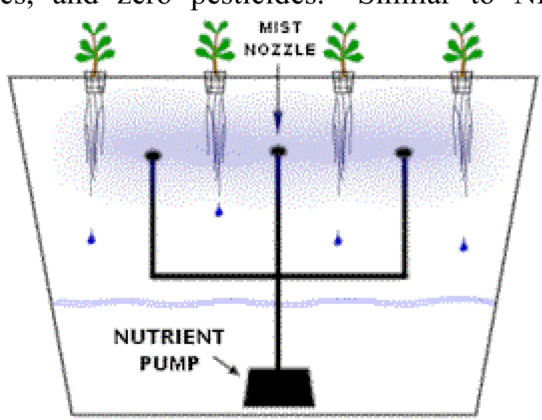

Figure 25: Aeroponic System diagram ("Aeroponic System," n.d.)

aeroponically are readily exposed to oxygen and require minimal growing media. However, misting heads tend to clog as a result of dissolved minerals in the solution, and misting interruption leads to plant death faster than NFT.

A fourth type of hydroponic system, wicking, involves using an absorbent material, like cotton, to transport nutrient solution from a reservoir to a growth medium surrounding the plant roots (“Hydroponic Systems 101,” n.d.). Some growth media actually suffice for wicking without use of a specified wicking material. As displayed in Figure 26, this system requires no moving parts (besides an optional air pump) and is relatively inexpensive. However, wicking systems provide little control of water flow and nutrient concentration, which can lead to nutrient build-up and lower plant quality (“Wick System,” n.d.).

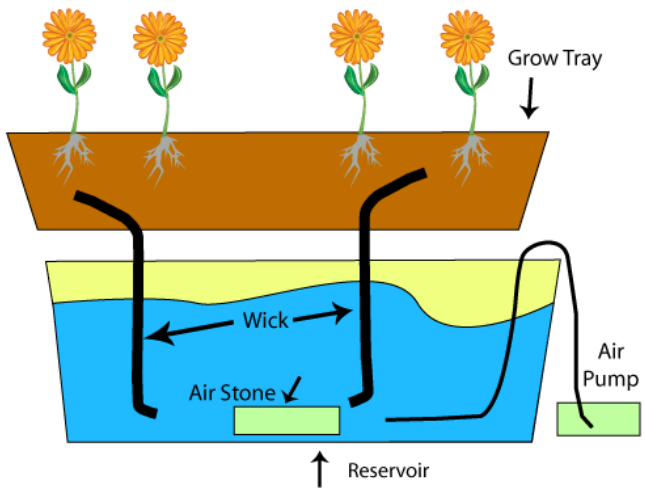

Figure 26: Wicking system schematic
(“Wick growing system,” n.d.)

Another commonly used system is referred to as ebb and flow (Figure 27). As the name implies, ebb and flow systems involve periodically flooding and draining plant roots with nutrient solution. Overflow tubes are used to set the desired water level height during flood periods. Disadvantages of the system include pH instability as a result of nutrient solution recycling and difficulty growing plants with low water resistance during flooding (“The Advantages,” 2011).

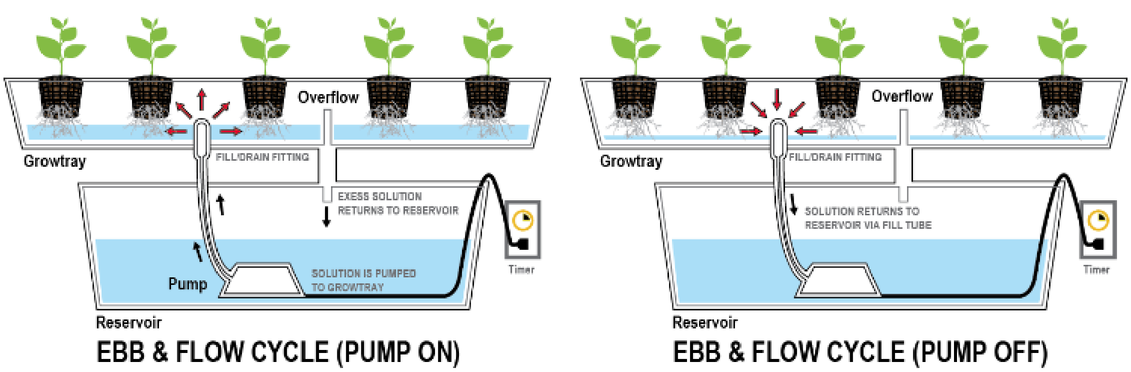

Figure 27: Ebb & flow hydroponic schematic (“Datko, S.,” 2012)

The final commonly used hydroponic technique is the drip system, shown in Figure 28, which involves a slow nutrient feed rate ("Hydroponic Systems 101," n.d.). The solution is pumped through tubing from a reservoir and dripped onto growth media below ("Hydroponic Drip System," n.d.). This method is widely used as it is relatively easy to install. Drip systems are best suited for plants having large roots that can soak up the solution more readily. The major downside of the drip system is frequent clogging issues caused by organic nutrient build up ("Hydroponic Systems 101," n.d.).

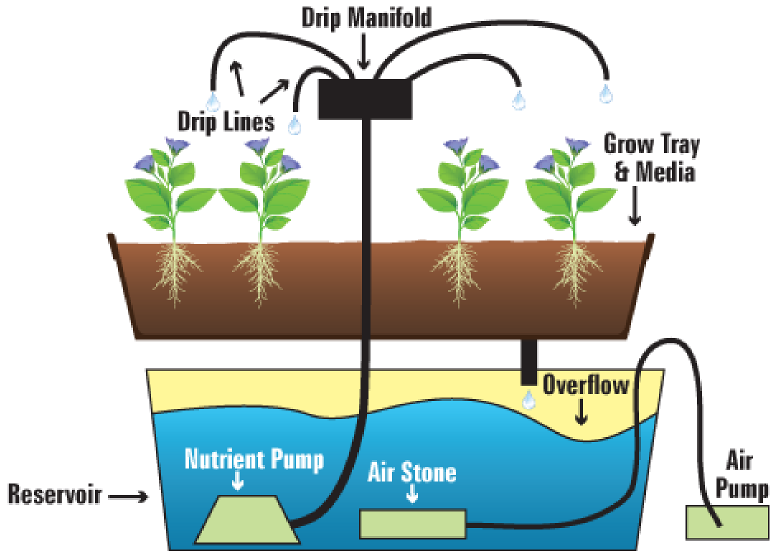

Figure 28: Drip hydroponic system schematic ("Hydro/Aquaponics," 2016)

Basic Greenhouse Designs

A wide variety of greenhouse designs are available to efficiently grow crops. This section will briefly discuss common types of free-standing greenhouses used for both small-scale and commercial applications. All greenhouse structures have pros and cons. The best greenhouse design for the task depends upon many key factors such as price, size, and durability requirements.

Three of the most common styles of greenhouse are glass, fiberglass, and plastic, seen in Figure 29. Glass can be used to fit a variety of frames and greenhouse shapes, including curves, slants, and straight sides. The main advantage of a glass style is its tight seal and barrier properties, resulting in better humidity and heat retention. However, glass structures are more easily damaged or broken, usually more expensive, and require a sturdy structure. Fiberglass covers are relatively lightweight and are quite strong; however, high quality, clear fiberglass grades are needed to allow for consistent, reliable light penetration. High quality fiberglass can cost just as much as glass. Plastic, on the other hand, tends to be much cheaper than glass or fiberglass and can be purchased for as little as one-tenth the cost. Plastics are capable of producing crops at a comparable quality to fiberglass and glass. However, they lack the durability of the other two styles and need to be replaced every year to every few years. Polyethylene is one of the most commonly used materials for greenhouse covers. It has a relatively low cost and weight and allows for good light penetration. However, its heat retention can be relatively poor, and UV deterioration occurs over long periods of sunlight exposure. Polyvinyl chloride plastic covers tend to last longer than polyethylene, but are also much more expensive (“Greenhouse Construction”, 2006).

Figure 29: Three examples of greenhouse covers from left to right: glass (“Cross Country Cottage,” n.d.), fiberglass (“Greenhouse Products, n.d.), plastic (“6 mil sheeting,” n.d.)

Like the cover materials discussed above, different types of frame structures, shown in Figure 30, yield distinct advantages and disadvantages. Common materials used in greenhouse frames are aluminum, iron, wood, and galvanized pipe. One frame style is referred to as the A-frame, which has a triangular shape consistent with its name. A-frames can be reinforced with diagonal bracing wires and are relatively easy to build. Another type of frame, the rigid frame, can be used in larger designs requiring a width of 30 feet or more; however, the design may yield little headspace, limiting the growth of plants. A third type, known as a panel frame, can be used in conjunction with plastic panels. While this construction is more labor-intensive and a relatively large amount of lumber is required, panel frames can be easily ventilated and easily taken down for storage.

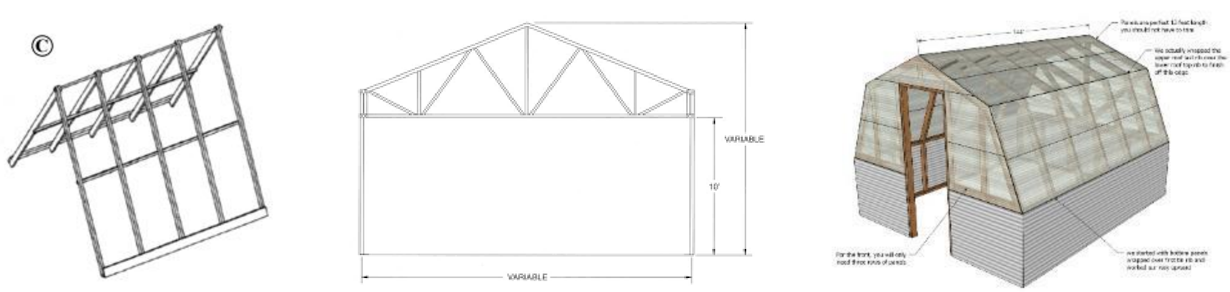

Figure 30: Three examples of greenhouse frames from right to left: A-frame (“Greenhouse Construction,” 2016), rigid frame (“The Quality Plus,” n.d.), panel (White, 2012)

Round-top frames, on the other hand, are usually made of metal, and have a rounded top as the name would imply. They are typically easy to build, cover, and ventilate relative to other models. One last frame structure is a pipe frame, which is commonly used for air inflated covers. It is very sturdy and uses differential air pressures to hold the inner and outer cover layers steady. Each frame style has a unique combination of strength, cost, and construction difficulty (“Greenhouse Construction”, 2006). Figure 31 displays these other two types of frames.

Figure 31: Two more examples of greenhouse frames, round top frame (left) and pipe frame (right) (“Greenhouse Construction,” 2006)

Greenhouse Modelling

Greenhouse modelling is a useful tool to better understand factors and phenomena affecting greenhouse performance. This section will discuss several models applied to estimate and quantify energy balances in greenhouses.

In their article from Solar Energy, Mashonjowa et al. discuss modelling energy in a naturally ventilated greenhouse growing roses in Zimbabwe. The article shows that an adaptation of the Gembloux Dynamic Greenhouse Climate Model (GDGCM) can yield reasonably accurate thermal performance results compared to empirical data taken on site. The GDGCM model incorporates differential equations used to describe heat and mass transfer phenomena. The parameters factored into the model are numerous, but key factors include the local environmental solar radiation intensity, outside temperature and wind velocity, material used for the cover, and heat transfer coefficient. The model includes eight heat energy balances to account for each layer in the greenhouse, including the soil, plant, air, and cover layers, and a mass balance to account for humidity. These balances make several assumptions, including the homogeneity of layers and verticality of fluxes. The only flux not assumed to be vertical was solar radiation. They use a program called the Transient System Simulation (TRNSYS v16) to solve the system of equations.

With these parameters, the system can calculate a year's simulation on a personal computer in under five minutes. However, this method is quite costly.

A relatively simple modelling approach was utilized by Silveston et al. in their article published in the Canadian Agricultural Engineering journal. They analyzed condensation heat losses and suggested methods to reduce them. This model involved an energy balance around the entire greenhouse system rather than a layer by layer approached. A water balance was also included to account for condensation heat losses. All heat transfer equations were at steady state. The associated system of equations was solved by successive approximation for specified environmental conditions. Once heating requirements were approximated, a cost estimate for heating equipment and fuel was given. Our team's model is based on this approach.

3.2 Micro-hydro Site Assessment – Trip 1

As outlined in the beginning of this chapter, multiple trips were made from the team's home base in Wellington to the project site in Horohoro. The first of these three trips was for assessment purposes and occurred from January 16 – 20, 2017.

Monday was mainly a travel day. We arrived on site in the late afternoon with project sponsor and Ngāti Kea Ngāti Tuara project manager, Eugene Berryman-Kamp. As Nathan and Paige had not been at the site since completing their IQP a year ago, and Aaron was completely new to the site, Eugene gave the team a brief tour. The first thing that Nathan and Paige noticed, in contrast to their last visit, was that the micro-hydro intake was completely unprotected, with any debris that came along freely flowing into the system, seen in Figure 32.

Figure 32: Unprotected intake upon arrival

The previous debris-catching grate and mesh structure had washed away in a storm and sunk to the bottom of the river. Eugene also pointed out a new structure in the river, downstream of the inlet but prior to the waterfall, a floating wetland dock. Eugene explained the anchoring system for this structure should we use a similar system to anchor the floating boom, which employs cables, waratahs (Y-shaped stakes), and a large eye-bolt that was twisted into the ground (Figure 33). Eugene even noted that if the water was deeper near the intake, they might have been able to use the wetland as a floating boom. However, the depth of the river in that area is relatively shallow during the summer months and would not suffice for growing the vegetation on the floating wetland.

Figure 33: Floating wetland and anchoring system (2017)

Next, Eugene brought the team down to the prospective greenhouse area where they are growing trees to be used in riparian planting, currently in the open air. Because the NKNT's recent funding application for a greenhouse had not been accepted, they decided to pursue a smaller, self-funded greenhouse. The materials were present but construction had not yet begun, seen in Figure 34. This smaller, self-ventilating greenhouse will serve to protect the plants in the coming autumn months. Eugene shared with us that they would still like to pursue a hydroponic greenhouse and showed us its potential plot, shown in Figure 35.

Figure 34: Greenhouse awaiting construction (January, 2017)

Figure 35: Potential hydroponic greenhouse plot (January, 2017)

The team continued to get acquainted with the site the next day, having more in-depth conversations with property manager and maintenance worker, Riki Oneroa. Riki explained to the team that currently they are growing the trees outside with no real protection beside from a mesh wind screen, seen in Figure 36. There is also a simple irrigation system in place, consisting of a hose and single rotating sprinkler head. There are four main areas of trees, each at different growth stages.

Figure 36: Native tree nursery area with 3 of 4 distinct growth stages visible

Next, Riki took us to the micro-hydro unit. The team noted the water level and asked how much this changes month to month. He noted that the water rises quite a bit in the winter months, from June to August. One of the team's main challenges became determining how to anchor the boom to account for these changes. During autumn, Riki explained that he has to clean the intake grate up to twice a day when the leaves are falling. We told him about our design concept for a self-cleaning, floating boom and Riki believed that this might work quite well for floating debris.

After speaking with Riki, the team was left to spend our own time becoming acquainted with the micro hydro system and intake. Our first task was to analyze the river flow, noting the water's behavior around the intake, which is summarized by arrows in Figure 37. The team took measurements, such as in Figure 38, pictures, and videos of the intake for use in the design process once we returned to Wellington.

Figure 37: River flow arrows

As seen in Figure 39, we found a large piece of scrap wood, about 6 meters long, and brought it into the river to test our idea of a floating boom, specifically if it could be self-cleaning as anticipated. The team threw debris into the water upstream to determine the anchoring angle of the boom for it to effectively deflect debris downstream along with the current.

Figure 38: Team members Aaron and Paige measuring the intake

Figure 39: Team member Nate examining the angle of the scrap wood boom test piece

With this test in mind, the team moved onto finding feasible anchoring points. Our original ideas concerning anchoring the boom consisted of:

A. Drilling pilings straight into the river bedrock.
B. Employing pilings on the shore, anchoring with rope within rigid tubing to maintain a constant distance from the shore and account for changing water level.
C. Using large rocks or other heavy objects to weigh down the boom.
D. Having one piling in an erosion rock downstream, and two pilings on shore upstream.
E. Hammering stakes into the shore with cables/rope running from the ends of the boom to the stakes, similar to the floating wetland setup.

The team also brainstormed other solutions besides the floating boom idea. These ideas included a mesh collection bag at the intake grate that could be easily lifted out of the water and emptied. This was deemed to be infeasible, as there already exists a metal mesh grating which currently sits out of the intake because it gets clogged too easily and inhibits flow to the turbines. The mesh would only cause similar problems and need to be cleaned just as often.

The next morning, the team spent the day in Rotorua at the office of Te Runanga o Ngāti Kea Ngāti Tuara, which is equipped with WiFi, unlike the project site. In an afternoon meeting with Eugene, we discussed our assessment of the site and potential solutions, in addition to the hapū's aspirations of constructing a commercial hydroponic greenhouse at the marae that would utilize energy produced by the micro-hydro unit.

In terms of anchoring of the boom, we learned that any permanent structure in the river may need to be approved by the many councils that have a stake in the river, including the Waikato Regional Council, Land Information New Zealand, Rotorua Lakes Council, and New Zealand Lands Trust. With this information, the team could rule out Option A, as drilling into the river bed would require going through the lengthy resource consent process, which takes months even should it go smoothly.

After getting into the river and having a better feel for the strength of the current flowing into the intake, the team could also rule out option C, as it became very clear that any structure had to be anchored onto the shore. This is supported by the example of the past intake grate being washed downstream as it was only wedged into the inlet with no onshore anchoring.

Eugene also informed us that drilling into the erosion rocks would not be a problem with resource consent issues, as they are not part of the river. The team initially thought that this might be the best option, drilling into an exposed rock (Figure 40) where the current splits the intake to have a piling on which the boom could move up and down with the water level. The upstream end would be anchored similarly to the floating wetland. With this idea in mind, the team tested the feasibility of drilling into an erosion rock the following day (Figure 41). Using a masonry drill bit with a 5/16 inch bit and a generator for power, we were able to drill into the rocks without issue. This proved to be a promising option.

Figure 40: Erosion rock that splits the river flow

Figure 41: Nate test drilling on erosion rocks on shore

While in Rotorua, the team looked back to their trip to Alden Lab, recalling their floating boom design and looking into modifying it for the hapū's needs. The initial basic design concept consisted of thick foam, a wood or plastic plank for structural purposes, and metal sheeting for siding. The next task was to source these materials, which could be done in Wellington the following week.

During this time at the Runanga office, the team was also able to meet more extensively with Eugene. He confirmed that we should be able to source materials in the Rotorua area, as it is quite industrial for a New Zealand city. He tasked himself with conversing with the district councils to see if there would be any issues with our construction and placement of a removable object in the river. We also talked through our plans to collect data, which would require the monitoring of power output and collection of debris to observe correlations between the two. He suggested we ask Riki if he would be willing to do this between trips to the project site, while the team was in Wellington.

As mentioned, we also spoke at length with Eugene about the native tree nursery and the hapū's aspiration of a hydroponic greenhouse. He informed us that they expect to operate the riparian tree nursery on a small scale, because a commercial tree nursery was not feasible. He again talked about the interest in a commercial scale hydroponic greenhouse to grow watercress. Currently, there is a need for hydroponically grown watercress, as when the plant is grown in the ground, it is grown in less than desirable conditions. Due to the geothermal activity in the area, the ground contains traces of toxins (arsenic) as well as contamination from farm runoff. There exists a market for hydroponically grown watercress in the Rotorua and greater Bay of Plenty region, as determined by the IQP in 2016.

Eugene was also able to take the team on a trip to a New Zealand hardware store chain, Bunnings Warehouse. We were able to see if they would have the basic materials for boom construction. Lumber and basic hardware were available, but sheet metal would need to be sourced from elsewhere. They did, however, offer a wide selection of fastenings, Y-stakes / waratahs, and wires/ropes to be used for anchoring. We picked up buckets for that debris collection to take place the following week.

Wednesday, January 19 was the team's second full day on site. The team wanted to examine the boom's effect on power output by first removing as many variables as they could, so they shut off the system to perform a thorough cleaning of the turbines, removing built up grime/algae (Figure 42 & Figure 43). We asked Riki if he cleaned the system often, and he said no since it did not affect the output. He did inform us that he will power-wash the penstock and give

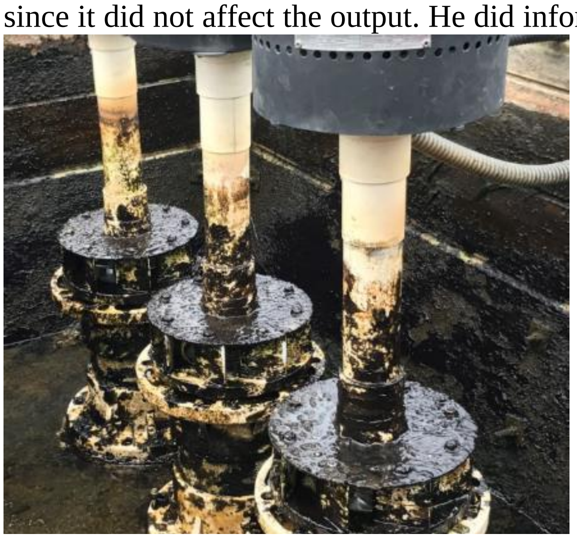

Figure 42: Turbines before cleaning

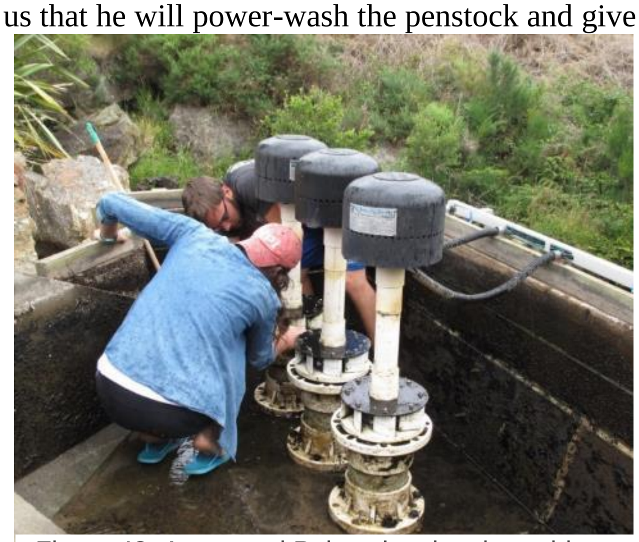

Figure 43: Aaron and Paige cleaning the turbines

the turbines a good cleaning once a year. We conducted the cleaning and discovered that Riki was correct, as it had no substantial effect on the power output, but it is important to keep the turbines clean enough to continue to run consistently.

With this knowledge, the team had to consider what material would be used for the piling and how it would be secured into the rock. Initial thoughts consisted of an adhesive such as epoxy or concrete. With the downstream anchoring idea shaping up, the team took another look at the floating wetland anchoring system. Riki showed us two types of pilings that were in the ground. One was a long, threaded eye bolt, drilled into the grown, shown previously in Figure 33. The other was a waratah, hammered into the ground with a sledge hammer (Figure 44). These both seemed like good possibilities.

Figure 44: Waratah (Bunnings, 2017)

On Friday, the team left the project site and was able to update Eugene with the week's progress and relay the data collection plans so he could inform Riki to collect the debris and keep track of the turbine output. We were also able to gain clarification of the use of the greenhouse, as it was very much a vague idea at the outset. We asked what we could produce that would be most helpful for them. Eugene asked for any basic requirements and early estimates with regards to cost and energy usage.

3.3 Floating Boom Design Process - Wellington

3.3.1 Boom Material Selection and Sourcing

The material of each component of the boom was selected to optimize the unit's longevity, stability, and strength, while keeping overall cost and maintenance to a minimum.

Closed-cell Foam

A closed-cell EVA (ethylene-vinyl acetate) foam, seen in Figure 45, was selected for the floatation component of the boom, given its low density (34 kg/m^3) and high UV resistance. The team sourced the material from New Zealand Rubber and Foam Ltd., a company based in Tauranga that delivered the material to the project site upon our second arrival to Horohoro. Candidate thicknesses of the foam were 40, 60, and 80 millimeters. The team selected the 40 millimeter thickness after consulting the calculations for buoyancy and stability to follow. Foam from this distributor comes in sheets 2.4 meters long and 1.2 meters in width, but can be cut to specifications within this range.

Figure 45: Foam strips to be used in boom

Siding

Material for the vertical siding needed to be smooth to allow for debris to travel along the length of the boom without getting hung up at any point. The siding material also needed to be relatively dense, to help partially submerge the foam and provide stability for the boom. Marine-grade 316 stainless steel was selected to serve this function, because of its high density (8,000 kg/m^3) and resistivity to corrosion, especially in aquatic applications. After visiting a local sheet metal shop in Wellington to view samples of varying thicknesses of the metal, the team determined 1 millimeter thickness to be ideal for our application. The 0.5 millimeter thickness was deemed too flexible given the length of the boom, while the 2 millimeter thickness was anticipated to be too rigid and heavy for this purpose.

Top Board

Several candidate materials were assessed for the board to be implemented above the foam. Initially we considered using a low-density wood, but this option was ruled out due to concerns for the longevity of the boom. Pressure treated wood, although it would provide a longer life span, was also ruled out due to environmental concerns regarding the chemicals used in pressure treating coming in direct contact with the stream. A rigid PVC board was determined to be the best option for this application, given its UV and water resistance and much longer life span. However, the final design did not include this component of the boom due to concerns for stability given its addition of weight above the water line.

3.3.2 Boom calculations

Buoyancy

Given a number of varying parameters for each of the boom's three components, the water level was calculated by equating forces of gravity and buoyancy to simulate a static state:

$$\Sigma F_{buoyancy} = \Sigma F_{gravity}$$

$$\rho_{H_2O}(Vg)_{foam} + \rho_{H_2O}(Vg)_{siding} + \rho_{H_2O}(Vg)_{board} = m_{foam}g + m_{siding}g + m_{board}g$$

Cancelling out gravity:

$$\rho_{H_2O}(V)_{foam} + \rho_{H_2O}(V)_{siding} + \rho_{H_2O}(V)_{board} = m_{foam} + m_{siding} + m_{board}$$

Substituting w * L * t for volume and w * t * L * ρ for mass:

$$\rho_{H_2O}L[w_{foam}(t_{board} + t_{foam} - h) + 2t_{siding}(w_{siding} - h)]$$

$$= L\,[(wt\rho)_{foam} + 2(wt\rho)_{siding} + (wt\rho)_{board}]$$

The calculation becomes per unit length, yielding:

$$\rho_{H_2O}[w_{foam}(t_{board} + t_{foam} - h) + 2t_{siding}(w_{siding} - h)]$$

$$= (wt\rho)_{foam} + 2(wt\rho)_{siding} + (wt\rho)_{board}$$

Where:

ρ = density

V = volume

g = gravity

m = mass

h = distance from top of boom to water level

w = width

t = thickness

L = boom length

Stability

The team recognized the importance of stability in the design for the floating boom. The degree of stability was calculated given varying parameters to ensure that the boom would not have the tendency to roll once installed. A benchmark for the degree of stability of a merchant ship had a metacentric height between 0.3-1.0 m was determined to be sufficient for our application according to Singh in his *Experiments in Fluid Mechanics*. The greater the metacentric height, the greater the stability. In comparison, Table 3 displays metacentric heights for varying vessels:

Vessel	Metacentric height [m]
Merchant ship	0.3 – 1.0
Sailing ship	0.45 – 1.25
Warships	1.0 – 1.5
River craft	Up to 3.5

Table 3: Metacentric heights for varying vessels (Singh, 2012)

To calculate the degree of stability, the center of buoyancy, center of gravity, and resulting metacenter must be determined first. The center of buoyancy was calculated by summing up the weighted center of gravities for each component of the boom and dividing this total by the total boom mass as shown in the equation below:

$$y_g = (m_{siding}y_{siding} + m_{foam}y_{foam} + m_{bolts}y_{bolts})/m_{total}$$

Where:

y_g = center of gravity

m = total mass for the specified component

y = distance from the reference point (bottom of the siding) in the y-direction to the center of gravity for the given component

The center of buoyancy was calculated using a similar method in which the weighted center of displaced water was divided by the total mass of water displaced. For this calculation, all materials were assumed to be impermeable to water, and the amount of material submerged was based on the waterline calculations described previously. Thus, the equation used was as follows.

$$y_B = (\rho_{H_2O}V_{siding}y_{siding} + \rho_{H_2O}V_{foam}y_{foam} + \rho_{H_2O}V_{bolts}y_{bolts})/m_{H_2O\ total}$$

Where:

y_B = center of buoyancy

ρ_{H_2O} = density of water

V = Total volume submerged in water for the specified component

y = distance from the reference point in the y-direction (bottom of the siding) to the center of displaced water volume for the specified component

The metacenter could then be determined using these parameters. In fluid mechanics, the metacenter is the intersection point between two lines connecting the center of gravity and center of buoyancy, as show in Figure 46 and Figure 47. The first line runs through the initial center of gravity and center of buoyancy, and the second line runs through the initial center of gravity and a new center of buoyancy resulting from a tilt in the vessel. This shift can be approximated using the least second moment of area for a given shape as demonstrated by Mansoor Janjua.

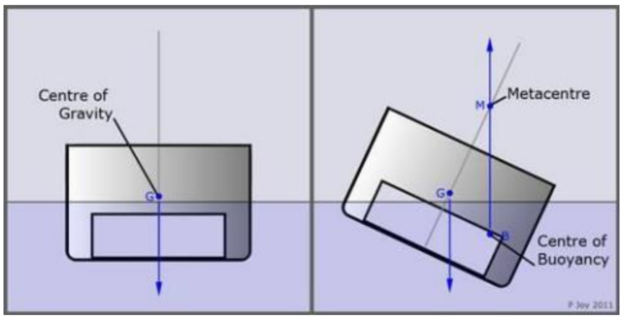

Figure 46: Visual representation of stability parameters ("Metacentric Height," 2016)

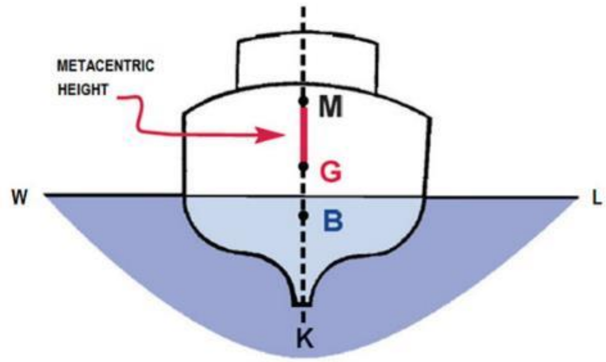

Figure 47: Metacentric height

The metacenter can be calculated using the following equation:

$$y_M = y_B + I_{AA}/V_{displaced}$$

Where:

y_M = metacenter

I_{AA} = least second moment of area for a rectangular shape

$V_{displaced}$ = total volume of displaced water

After finding these three parameters, the degree of stability, otherwise known as the metacentric height, can be estimated by simply subtracting the center of gravity from the metacenter:

$$H_{metacentric} = y_M - y_g$$

Due to concerns regarding the stability and flexibility of the boom following our initial calculations, the team refined the design by eliminating the top board of the boom all together. In doing so, we were able to achieve a much greater stability. The boom would also be less rigid and thus able to bend according to flow in the stream. With the new design involving only two major components, the foam and metal siding, the determining factor for the calculations to follow was the desired siding height above and below the water level. The team took into consideration the relatively low depth at the micro-hydro's intake, specifically where the boom was to be installed, and determined that the siding was to be 12 centimeters in height, with 6 centimeters submerged and 6 centimeters above the surface of the water. Again setting the forces of gravity and buoyancy to be equal, we were able to calculate the location of foam relative to siding that would yield the desired height above and beneath the surface.

$$\Sigma F_{buoyancy} = \Sigma F_{gravity}$$

$$(\rho V g)_{foam} + (\rho V g)_{siding} = m_{foam} g + m_{siding} g$$

$$\rho g[(V_{foam} + V_{siding}) = g(m_{foam} + m_{siding})$$

Substituting L * w * t for volume, with t = 6,

$$\rho[w[6 - (x + y)]]_{foam} + 6(w)_{siding}] = (wt\rho)_{foam} + (2wt\rho)_{siding}$$

Where:

$x =$ height of foam above water level [cm]

$y =$ height of siding above foam [cm]

$w =$ width

$t =$ thickness

$\rho =$ density

L = length of boom

With the refined design, we were able to meet our goal of achieving the stability of a small seagoing vessel. The metacentric height for the refined design was 0.43 m, not yet accounting for any hardware to be added to the design.

3.3.3 Final Design

Following the decision to eliminate the top component of the boom, the challenge then became how to fasten the foam and siding without adding excess weight above the waterline. To achieve this, we selected 316 stainless steel M8 threaded rod, which would be implemented above and below the foam every 80 centimeters for the length of the boom. With the rods spanning through the sheet metal, nuts would be implemented on the outside and inside of the siding, holding the sheet metal at fixed locations along the threaded rod. Five 1-meter lengths of threaded rod were cut in Wellington to yield 20 sections, each about 240 mm in length after the cuts had been made and ends sanded to restore the threads.

The final design for the boom, depicted in Figure 48, developed using the above calculations for buoyancy and stability, consisted of the following components:

- Six 316 stainless steel sheets: 1 mm thick, 120 mm wide, 2.4 m long
- Three sheets of EVA foam: 40 mm thick, 220 mm wide, 2.44 m long
- Five meters of M8 316 stainless steel threaded rod, cut into 20 pieces ≈ 24 cm long
- Forty M8 316 stainless steel hex nuts
- Forty M8 316 stainless steel nylon-insert lock nuts

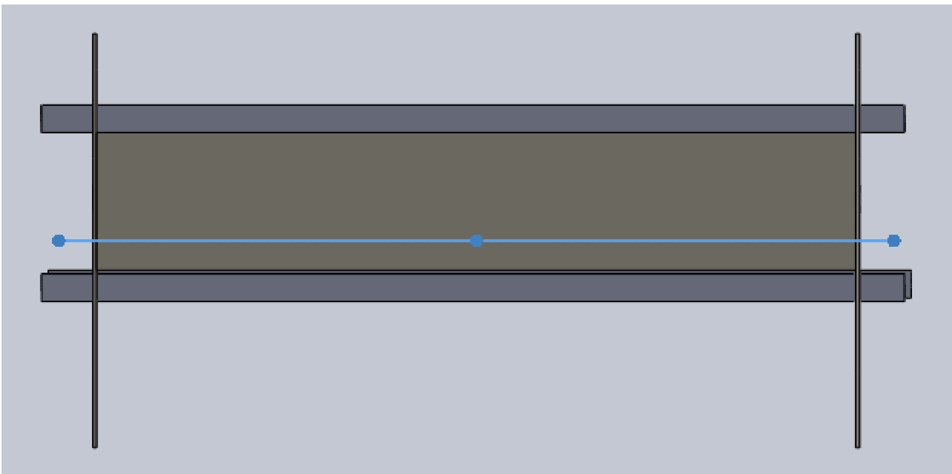

Figure 48: SolidWorks rendering of the boom and water level

3.4 Boom Construction and Installation – Trip 2

The construction of the boom was conducted during the team's second trip to the project site in Horohoro. Eugene brought us to Bunnings Warehouse and Sheetmetal Industries, Ltd. to pick up hardware, anchoring materials, and sheet metal in Rotorua. Construction began thereafter at the project site in Horohoro.

The first step in constructing the boom was measuring the hole locations for the threaded rod in the stainless steel sheets. The hole locations reflected the buoyancy calculations and final design developed by the team. Forty millimeters separated the top and bottom rows of threaded rod to allow for the insertion of the EVA foam between the rods. The center of the top row of bolts would be 24 millimeters from the top edge of the stainless siding, with the bottom row 72 millimeters from the same top edge, leaving exactly 40 mm between the inserted bolts. The team deemed 10 millimeters to be an appropriate minimum distance from the edge of the stainless siding to the edge of any hole, including those on the ends of the boom and those where the sheet metal would overlap at each of the three sections. After these marks were made and double checked, Aaron began prick punching these locations in preparation for drilling, seen in Figure 49. Nate drilled holes with an M8 size drill bit in the stainless steel. Four stainless steel eye bolts were to be installed on each end and each side of the floating boom for anchoring purposes. Although the calculated water line for the boom was closer to the bottom row of bolts, the eye bolts were placed at the midpoint between the two rows, to account for any variation

Figure 49: Aaron prick-punching the sheet metal

Figure 50: Nate drilling the stainless steel

between theory and reality and ensure that the boom would not be anchored from beneath the water level.

Once the stainless steel sheets had been marked according to the aforementioned specifications, they were carried to an area where the drilling would occur. The team used a prick-punch to make divots in the sheet metal to guide the drill bit and prevent it from sliding away from the correct hole location. Nate began drilling the holes, seen in Figure 50, first with a smaller bit to create a "pilot" hole in the interest of preserving the M8 bits needed to complete each one. Oil was used to keep the bits cool during drilling while maintaining a low drill RPM to keep cutting speed relatively low. After all 44 holes had been drilled, only one of the two 8 mm HSS drill bits purchased by the team had been burned out, which was a testament to the precautions taken to preserve the bits. Paige sanded the backside of the stainless steel with course sandpaper on an electric sander to smooth out the surface surrounding each hole.

With the stainless steel siding prepared, the threaded rod and nuts were inserted to conjoin both sides and each section of the boom (Figure 51). Four nuts were employed on each piece of threaded rod: locking hex nuts on the outside of the siding and standard 316 stainless hex nuts on the inside. This would allow the threaded rod to serve as spacers between the siding so that the EVA foam would not have to bear any load across its width in the horizontal direction. The sections were joined such that the siding would overlap in the direction of the flow along the side that would deter debris, so that no point existed that may catch debris along the length of the boom. The four eye bolts were installed, two at each end, using locking hex nuts. The EVA, closed-cell foam was inserted between the top and bottom rows of bolts and secured using nylon cord tied along the top row and at each end of the boom (Figure 52).

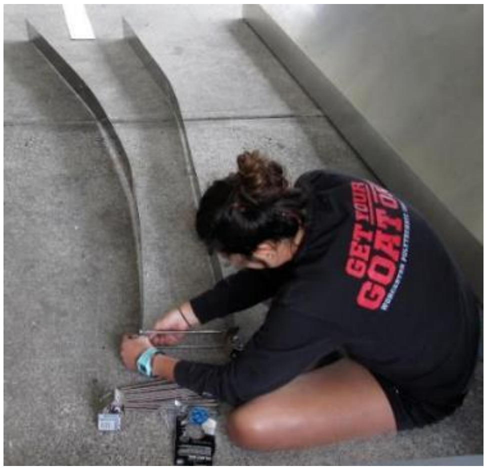

Figure 51: Paige beginning boom assembly

Figure 52: Nate tightening the nylon cord

The boom was anchored using three 0.8 meter waratahs, galvanized bow shackles and rope. Two waratahs were placed upstream of the boom and on opposite sides of the stream, with the third on the opposite bank as the intake, downstream of the boom. A pre-existing piling that served as the end of a fence surrounding the intake was used as the final anchoring point on the downstream end. The waratahs were driven into the banks with a sledgehammer, with shackles and rope connecting them to the boom. Each shackle has a working load limit of 330 kg. The 8 millimeter diameter rope has a breaking strength of 1,000 kg, but will likely need replacing after anticipated wear and tear. Figure 53 displays the boom after its initial installation at the end of the team’s second trip to the project site.

Figure 53: Boom's initial installation, anchored in front of the intake

With the boom in the water, the team was curious to see if it was floating at the calculated level. Figure 54 shows the water height on the boom shortly after its initial placement into the stream. It measured in at around 6.8 cm, very close to our anticipated 6 cm water line.

Figure 54: Waterline on the boom

3.5 Boom Design Refinement – Trip 3

3.5.1 Assessment

During Week 6, the team returned to the project site for their final trip to assess the effectiveness of the boom. There was a large rainstorm that came through the area in the days leading up to this trip and the team was curious to see the status of the boom after the severe weather. When we got to the site, we discovered that the foam on the upstream side of the boom had dislodged due to the heavy flow caused by the storm. The leading edge of the boom, without a sort of "bow" to protect it in heavier flows, had a tendency to submerge, adding a downward force to the foam and causing it to be dislodged, seen in Figure 55. After consulting with Riki regarding this problem, we decided a nose piece installed on this upstream end of the boom would prevent this from recurring. The

Figure 55: Dislodged foam after storm

nosepiece would divert water around each side of it, leaving the foam undisturbed by the water flow. In addition to the nosepiece, more nylon was added to the design, which now included 3 strings along the top and two along the bottom to make sure it was secured (Figure 57). The water level on the boom had rose about 1 cm since the last visit, which was attributed largely to the upward bowing of the foam pieces between sets of bolts along the length of the boom. Figure 56 displays this waterline, just over hallway up the boom. In addition, the team also decided to install a mesh screen to catch submerged debris.


Figure 56: Water line after 1 week


Figure 57: Electric tape around threaded rod to protect nylon

3.5.2 Design Modifications

With this idea in mind, we thought about the shape of the nosepiece that would allow it to best serve its function. Considering manufacturability and durability, the team decided to simply bend a piece sheet metal into a rounded shape, as completely folding the metal into a v shape would create a point of weakness and be more difficult to attach to the existing boom design. The team conducted an elementary calculation to determine the length of the metal sheet needed to cap the end:

$$1/2\, C = \pi r$$

Where C is the circumference and r is the radius, which is the width of the boom. With this calculation, the team determined the minimum length of the nosepiece to be 35 cm, but considering the length needed to overlap the siding to fasten the piece, we decided 50 cm would be an appropriate length.

The team was able to get into town to the sheet metal company that had originally provided the siding for the boom, Sheetmetal Industries Ltd., where we were able to have a piece cut to serve as the nosepiece for the floating boom. The piece was the same thickness and width as the siding (1 mm and 120 mm,y) respectively, and 50 cm in length, as determined. While in Rotorua,

Figure 58: Addition of the nosepiece and extra nylon

the team also purchased more nylon cord and electrical tape to minimize the upward bowing of the foam sheets between bolts along the length of the boom. The result of these additions can be seen in Figure 58.

Given the inability of a floating boom to prevent submerged debris from entering the micro-hydro's intake, the team decided to supplement the floating boom installment with a mesh screen that would extend from the river bed to the river surface and thwart any submerged debris from entering the system's intake. To accomplish this, the team considered several options. Initially, we intended to fasten the mesh screen to the boom to achieve a self-cleaning angle without the need for additional anchoring on shore. However, after considerations for the functionality of the boom under flood conditions, given that the mesh screen would be anchored to the river bed and might sink or warp the boom in this case, we decided to install the mesh screen independently, but at a similar angle and directly behind on the intake side of the boom. To do so, two additional 1.5 m waratahs were purchased for anchoring, along with rope and shackles to secure the top edge of the screen. After measurements of the water depth at this location were taken, the team folded the mesh twice over itself for strength, still leaving ample length in accordance with the measurements taken, and installed 10 brass plated grommets equally spaced along the top of the 5 meter length of the mesh (Figure 59).

Following the installation of grommets and anchoring materials, the mesh screen was ready

Figure 59: Mesh before and after grommet addition

to be implemented. Because drilling into the riverbed would require resource consent from several local councils, the team chose to anchor the mesh on the bottom of the stream using large rocks left over from the micro hydro construction. With these in place, the screen was pulled from both ends to the two waratahs installed on the river bank, and pulled taught by another length of rope running from end to end along the mesh and through the grommets which had been installed in the folded top edge. Figure 60 displays the mesh installed and being anchored with erosion rocks.

Figure 60: Mesh being held down by rocks

With the mesh in place, the micro hydro intake was conceivably immune to debris, both floating and submerged. However, the screen was not self-cleaning like the boom, and after becoming less porous with debris buildup over time, would dip beneath the surface due to the consequential increased force on the unit. To mitigate this effect, the micro hydro intake gate could be temporarily closed, which stops flow to the intake, allowing the mesh screen to be cleared by the natural flow of the stream parallel to it. After this has been done, the top edge of the screen returned to its position above the surface of the water, allowing it to function properly again. The morning before leaving the site, the team also decided to cut up the extra piece of skinny foam to insert into the mesh to help keep it afloat (Figure 61). Figure 62 and Figure 63 show the boom in the water with the nose piece and the final configuration.


Figure 61: Mesh and boom system


Figure 62: Nose piece


Figure 63: Full view of intake

3.6 Post-Installation and Final Design Refinements – Trip 4

On March 17, team member Paige returned to the project site to conduct a post-installation assessment of the boom. The area had just endured a 20-year storm, with a heavy deluge of rain. According to Eugene, there was a month's worth of rain in one night. This wreaked havoc on the stream with flood waters rising over a meter, seen in Figure 64. As expected with a storm of this magnitude, the rocks holding down the mesh had dislodged and the mesh was now flowing freely in the water, no longer stopping any debris. However, before the storm, the mesh was catching so much submerged debris that it was being pulled underwater. To clean the mesh, Riki closed the intake to create a back-washing effect and allowing the mesh to be cleared with the current as the water was no longer rushing into the intake.

Figure 64: Flood level waterline

Upon Paige's arrival to the site, the boom was sitting on the bank of the stream out of the water. Riki had removed the boom after the storm, and its far-side lines were detached. While the boom was anchored in the water, these lines were submerged, and pulled along with the current, catching a great amount of debris, especially in the storm waters. An example of the debris build-up can be seen on the cable wires that anchor the floating wetland, located just downstream (Figure 65). This large amount of debris in combination with the flood waters caused one waratah to dislodge from the far bank. The other waratah on the far bank was more firmly in place, however the rope could not be pulled through the bow shackle as easily as designed, so the rope was untied and let go to the other side of the river. The debris that the far-side lines caught also put the boom under great shear stresses, causing deformation. The stream side of the boom attached to the far-side lines was pulled so much that the threaded rods were no longer perpendicular to the sheet metal siding (Figure 66).

Figure 65: Debris after flood on line

In addition, the piece of foam that had dislodged and been severed by the sheet metal siding after a small storm in the week following the boom's initial implementation was now completely broken off (Figure 67). Fortunately, there were two extra pieces of foam that we could use as replacement piece. In doing so, the nose piece had to be removed and the end of the boom partly disassembled. Replacing this foam proved to be a more difficult task than initially thought. The nylon lines that run above and below the piece were challenging to maneuver and got tangled up with the installation of the replacement foam piece. After the foam was back in place, the lines needed to be straightened out and untangled. The nylon's force from threaded rod to threaded rod also caused significant bowing of the sheet metal siding. We discovered the nylon to no longer be long enough with the boom's new shape. Wire ties were used as an extension to attach the end of the nylon to the last threaded rod.

Figure 66: Boom deformation after flood

Figure 67: Broken foam

With the boom as well-repaired as it could be, it was returned to the river in working condition (Figure 68). Unfortunately, because of the storm waters, no data was taken as the system had to be shut down in the week leading up to Paige's visit. However, in speaking with Riki, he said that the boom was doing its job and there was much less floating debris getting to the intake grate. NKNT is also in the process of installing WiFi at the marae. Once this happens, power output will be able to be monitored remotely.

Figure 68: Boom back in the water after repairs

3.7 Greenhouse Modeling

During the team's time in New Zealand, we reached out to local hydroponic specialists that had experience growing watercress. One of the most helpful people we were in contact with was Neville Stocker, technical director for PGO Horticulture LTD. In addition to conversing with him through email, team member Paige was able to visit his business in Tirau, a small town west of Rotorua, and have a face-to-face interview with Neville on March 23, 2017. His expertise and advice is referenced throughout this section.

3.7.1 Energy Balance

For optimum plant growth, the temperature must be maintained within a certain range. While New Zealand's climate is relatively moderate compared to many parts of the world, the temperature still dips below 10 degrees Celsius in the winter, and frosting is a concern on particularly cold nights according to World Weather Online ("Rotorua Monthly Climate," 2017). Thus, we have performed design calculations to estimate the heating requirements a theoretical greenhouse having the appropriate dimensions for the plot of land in Horohoro.

For this calculation, previous literature demonstrates several methods of estimating heating costs for greenhouses as described in Section 2.4. Our group decided to pursue a quasi-steady state approach that performs a total system heat balance rather than a layer by layer as described by Silveston et al. A system of differential equations was solved that includes a water vapor balance, a total energy balance, and two energy balances on the double layer shell.

Since the humidity should be controlled for optimum plant growth and significantly changes the specific heat of the air, a water vapor balance was performed that accounted for the water vapor entering the greenhouse via air circulation and transpiration and via air circulation, condensation, and dehumidification. The resulting balance is shown below.

$$M_{wi} + M_{w3} = M_{wo} + M_{w4} + M_{w5}$$

Where:

M_{wi} = total water vapor entering the greenhouse via air circulation

M_{w3} = transpiration rate

M_{wo} = water vapor leaving the greenhouse via air circulation

M_{w4} = water vapor removed via dehumidification

M_{w5} = water vapor condensing on the greenhouse shell

The total energy balance around the system assumes that all energy entering the greenhouse either exit or be absorbed into items inside of the structure, such as the soil or air. The heat leaving the greenhouse can be categorized into three main types of heat loss, namely radiation, condensation, and convection. Thus, the total heat balance can be approximated by the following equation:

$$S_1 = L_1 + L_2 + L_3 + M_a C_p (t_I - t_E) + Q_g - \lambda (M_{w4} - M_{w3})$$

Where:

S_1 = heat input required to maintain temperature t_I

L_1 = convection heat loss

L_2 = condensation heat loss

M_a = mass of air in the greenhouse

C_p = specific heat of air in the greenhouse

t_I = internal temperature of the greenhouse

t_E = external temperature

Q_g = heat loss to the soil

λ = latent heat of condensation

A double paned plastic shell, consistent with Silveston et al., was chosen for this estimate. Since the temperature differs significantly on each side of the cover, a shell balance around each side was performed. For the inner layer, heat gains from radiation, condensation, and convection inside the greenhouse were set equal to radiation and conduction heat losses to the outer layer. The overall balance is shown below:

$$h_I(t_I - t_{g1}) + \lambda k_c(C_{am} - C_A) + \sigma F(t_I^4 - t_{g1}^4) = \frac{k^*}{x}(t_{g1} - t_{g2}) + \sigma F(t_{g1}^4 - t_{g2}^4)$$

Where:

h_I = the interior convective heat transfer coefficient

t_I = interior temperature

t_{g1} = temperature of the inner cover layer

k_c = convective mass transfer coefficient

C_{am} = mean absolute humidity

C_A = the absolute humidity

σ = Stefan-Botlzmann constant

F = radiation view factor for the greenhouse shell

k^*= the thermal conductivity of air between two plastic films

x = distance between the plastic films

t_{g2} = temperature of the outer cover layer

Radiation view factors were approximated for a given greenhouse geometry and plastic transmissivity. A full explanation for the radiative view factor is cited in the appendix of Silveston et al. For the outer layer, conduction and radiation heat gains from the inner layer are equated to convection and radiation heat losses to the environment. The resulting equation is shown below:

$$\frac{k^*}{x}(t_{g1} - t_{g2})x + \sigma F(t_{g1}^4 - t_{g2}^4) = h_E(t_{g2} - t_E) + \sigma F(t_{g2}^4 - t_{sky}^4)$$

Where:

h_E= external convective heat transfer coefficient

t_E = outside temperature

t_{sky}= temperature of the deep sky to which heat is radiated

MathCad was used to solve these four questions for four unknown variables, S_1, M_{w4}, t_{g1}, and t_{g2} for specific atmospheric conditions chosen to best represent each month of the year based on weather data available for the region. For each month, a day and a night set of conditions was utilized, resulting in 24 atmospheric conditionals each representing approximately 15 days. This process was repeated for combinations of windy, calm, cloudy, and clear conditions. By summing the total heat requirement for each time period, a total annual heat requirement was estimated to maintain optimal growing conditions for watercress. A separate heat total was reported for each winter month since heating during cold months will be more critical. Additionally, heating may be unnecessary during summer months.

Discussion of Inputs

Weather

For each time period, the temperature, humidity, cloud cover, and incident radiation was adjusted based on available data. Temperatures, humidity, and cloud cover data was obtained from World Weather Online for 2016 and applied to this simulation. The monthly high and low temperature values were used to represent the daytime and nighttime temperatures for the model, respectively. Average humidity and cloud cover percentage values were reported for each month, and were used for both the daytime and nighttime inputs for the model. While we acknowledge that these values the humidity and cloud cover will change throughout the day, data for the average humidity and cloud cover for each month was not available.

Radiation Terms

Incident solar radiation values on a horizontal surface throughout the year at 40° N latitude were taken from the ASHRAE Handbook of Fundamentals as cited in Cengal & Ghahar, 2015. Since Horohoro is located at 38.2° S, these values were assumed to be reasonably accurate. Values were reported for each of the four seasons at this latitude, one for the month of January, April, July, and October. Hourly incident radiation values given in the table were averaged over a period of 12 hours to determine an average daily radiation value that was input into the model. It is important to acknowledge that incident radiation values do vary throughout the day, but an average was assumed to be appropriate for the model in keeping with the quasi-steady-state approach for 24 time periods. Since this table reported seasonal radiation values for the northern hemisphere, our model switched the January and July data as well as the April and October data to account for the seasonal difference between hemispheres. For each cloud cover input, a Cloud Cover Factor (CCF) was reported following recommendations from "Solar Radiation on Cloudy Days," a paper written by K. Kimura and D. G. Stephenson in conjunction with the National Research Council of Canada. In this paper, a plot of CCF with respect to cloud cover was generated, and our team interpolated on this model to estimate the CCF for the average cloud cover for a given month. This CCF was multiplied by the Incident Radiation for the simulations. This model was validated in the Kimura and Stephenson's study for weather in several major Canadian cities and was found to be reasonably accurate. Transmissivity and absorptivity values for polyethylene were taken from Pieters & Deltour, 1997.

For radiation terms between layers of the greenhouse, the view factors used were based upon the geometry of the system. For radiation between the two layers of the cover, a view factor of 0.9 was applied with the assumption that the layers behaved as infinite parallel planes with an emissivity of about 0.9. For radiation interactions between the cover and the internal greenhouse air, a view factor of 0.58 was used. This view factor was also used to approximate radiation between the ground and the cover. Details for this calculation are referenced in Silveston et. Al. This procedure approximates this grey body view factor by using direct radiation view factors for a greenhouse represented by half of a cylinder, where the flat plane represents the plant mass, the ground is parallel beneath, and the cover is the curved portion of the cylinder. The emissivity for both the plant mass and the plastic shell was approximated to be 0.9 based on their study. Radiation view factors between the outer cover layer and the sky was assumed to be unity.

Convection Terms

Convective terms included interior convection on the inner cover layer and exterior convection on the outer cover layer. For both convection terms, the convective heat transfer coefficient was taken from the ASHRAE Guide and Data book per the method of Silveston et al. For this approximation, the interior convective heat transfer coefficient was found to be 7.4 $W/m^2/K$, and the exterior coefficient was estimated to be 9.1 $W/m^2/K$ for still air and 34.1 $W/m^2/K$ for a windy condition of 28 km/h.

Conduction Terms

For the cover layer heat balances, a conductive heat transfer coefficient for the air between the two plastic layers was estimated based on empirical data. The resulting effective conductive heat transfer coefficient was approximately four times the conductivity of still air. Thus, a value of 0.10 W/m/K was used for a distance of 25 mm between plastic layers.

Condensation Terms

Condensation heat loss was approximated by multiplying the latent heat of condensation by a mass transfer coefficient, the difference in absolute humidity between the bulk greenhouse air and the air directly above the inside cover, and the area of the cover. The mass transfer coefficient for condensation was calculated by Silveston et al. by applying j-factor correlations. For this calculation, the internal air velocity was assumed to be 0.5 m/s. The resulting coefficient was found to be consistent with ASHRAE data. The absolute humidity at the greenhouse cover was calculated by multiplying the relative humidity by the maximum absolute humidity for the temperature of the inside greenhouse cover. The same method was used to determine the absolute humidity of the interior for the specified interior temperature.

Water Vapor Balance Terms

For the water vapor balance, the only unknown was the amount of water that needed to be added or removed by the humidification or dehumidification to maintain a given internal relative humidity. All other quantities were estimated from known data. The rate of condensing water on the cover was found by multiplying the condensation mass transfer coefficient by the area of the cover and the difference in absolute humidity for the cover temperature and the interior bulk temperature. The evapotranspiration rate was based upon research by Silveston et al., which reports that, on a sunny day, the evapotranspiration rate reaches 0.66 mm H_20/h, and at night the value drops to roughly 0.05 mm H_20/h. This value was converted to kg/s using conversion factors discussed in the FAO Corporate Document Repository in their Introduction to Evapotranspiration page ("Chapter 1," n.d.).

3.7.2 Recirculation System

In section 3.1.3, six different commonly used hydroponic methods were discussed. After conversations with hydroponic greenhouse experts, we have chosen to utilize the nutrient film technique (NFT) for this watercress design. This method yields high quality lettuce strain as a result of tight nutrient control and a reasonable amount of maintenance. Since the NFT approach was chosen for this hydroponic system design, a water recirculation system must be implemented. As discussed previously, water is pumped to the top of each channel and nutrient solution flows down the incline, delivering nutrients to each of the plants.

Our team initially tried to calculate the water requirements and recirculation rates based on the uptake rate of nutrients in watercress, but, after speaking with NFT experts, a better approach was adopted that focuses on heuristics. Over the last few decades, rules of thumb have been established for water flows and circulation rates for watercress grown hydroponically. Additionally, the nutrient film technique involves maintaining a specific water level that only submerges the base of the roots in nutrient solution, allowing the remainder of the roots to be naturally oxygenated from the air. Thus, Neville recommended a set of values for a system having the dimensions we specified. Furthermore, he recommended specific materials and parts to construct the system. Additional research was performed online and other hydroponic experts were consulted to find more information. Our estimate for annual water requirements are based on these recommendations.

3.7.3 Electricity Requirements

One of the original motivating factors for constructing a greenhouse was to utilize excess energy produced by the micro hydro unit. Ideally, the greenhouse could run solely on the micro hydro unit's energy. Thus, determination of the electricity requirements for this greenhouse is an important step in this engineering feasibility assessment.

The first step in this estimation was to establish which components of the greenhouse will require electricity and how much electricity they will use. The electrically active components identified by our team included the water pump, pH monitoring system, water heating equipment, and air heating equipment (if necessary). For each component, the electricity requirements were specified in the product's information. The wattage was then multiplied by the approximate amount of annual run time to achieve the estimated total electricity requirement.

Nutrient Solution Pump

A small pump will be required to carry the nutrient solution from the bottom of each slightly pitched table back to the top. For the purpose of this calculation, we are assuming three 15 meter long tables, each 1.2 meters in width to be employed within the greenhouse. A 3% grade is typical in such applications, meaning each table will drop 45 centimeters along its length, but head losses will be assumed to be 1 meter. To size the pump, the method described in University Upstart article “Sizing a Pump for Hydroponics or Aquaponics” was used. In this method, the total flow rate required and head required are used to read a pump curve from a supplier such as Active Aqua. The flow rate is estimated based on the number of gullies used and a heuristic for the flow per gully. In this case, a heuristic of 4-6 GPH was used for our assumption of 25 gullies, resulting in approximately 100 – 150 GPH requirement.

Heat Exchanger

Because the nutrient solution must be heated and within a certain temperature range, a heat exchanger will be necessary to maintain this temperature within the tank. The tank is assumed to be 450 liters. Optimum temperature for the nutrient solution is 16 degrees Centigrade, but water in the tank will be assumed to be 18 degrees in anticipation of convective heat loss as the solution flows down the 15 meter long tables. Heat needed to maintain this temperature within the tank can be estimated by summing the heat lost to conduction through the tank and convection as the solution travels down the tables and returns to the tank. For a barrier of constant thickness, such as the 450 L tank, conduction is defined as follows:

$$\frac{Q}{t} = \frac{[kA(T_{hot} - T_{cold})]}{d}$$

Where:

$\frac{Q}{t}$ = heat transferred/time

k = thermal conductivity of tank

A = area of the conductive surface

T_{hot} = solution temperature = 18 degrees C

T_{cold} = ambient greenhouse air temperature

d = thickness of tank walls

The heat lost to forced convection as the solution travels down the pitched tables can be estimated using the convection equation.

$$\frac{Q}{t} = h_c * A * (T_{hot} - T_{cold})$$

Where:

$\frac{Q}{t}$ = heat transferred/time

h_c = convective heat transfer coefficient

A = area of the convective surface = 54 m^2

T_{hot} = solution temperature = 18 degrees C

T_{cold} = ambient greenhouse air temperature

Although other forms of heat transfer exist in this circumstance, summing the heat lost to forced convection down the tables and conduction through the tank will result in a good estimate for solution heat loss with which we can estimate energy usage and provide recommendations for a heat exchanger to maintain an ideal solution temperature.

3.7.4 Cost Estimate

After the heating, recirculation system, electricity, and structural requirements were calculated, a cost estimate for the entire system was estimated. Equipment was specified and a cost estimate was provided based on research online and emails with vendors. A cost estimate for electricity was also provided based on a data from NKNT electric bills. The total cost for each of the elements analyzed in this paper was summed to estimate a total cost that excludes operational labor and project management costs.

Chapter 4: Results and Discussion

4.1 Boom Results

Our team successfully designed, constructed, and implemented a floating boom and mesh system that deflects floating debris downstream and catches submerged debris without negatively affecting flow into the turbine system inlet. A demonstration of the floating boom in action is shown in Figure 69. Floating debris approaches the boom, slides along the sides, and continues downstream.

Figure 69: Boom in action

The images above highlight the effectiveness of the floating boom. However, we acknowledge that for the demonstration above the boom had not yet been anchored. The anchor lines to the opposite side of the stream did collect some debris, but this was addressed later in the project and these two anchor points were removed. Thus, the final design does not catch significant levels of debris on the anchoring lines.

The floating boom's waterline level slightly varied (about 1 cm) from the intended waterline that was used to calculate the appropriate height of foam relative to the siding. However, the boom did still function well sitting slightly lower in the stream, and there was still sufficient siding above the surface of the water to prevent debris from going over the structure. Given that closed-cell EVA foam absorbs virtually no water, this difference between theory and practice was attributed to the foam bowing slightly upward between pairs of threaded rods along the length of the boom, raising its center of buoyancy. The boom also proved to be stable, even in stormy conditions.

In addition to the success of the boom, the mesh effectively caught submerged debris as shown in Figure 70. When the mesh system became congested, Riki was able to flush it by closing off the inlet and allowing backpressure to wash off the debris. The suction returned upon reopening the inlet.

Figure 70: Debris on mesh

The Pokaitu Stream at the project site is subject to varying conditions. For one, the stream must pass through a series of farms before reaching the marae. The farming activities vary daily, and so does the debris washed into the stream. The river's conditions are also highly dependent on the weather, which changes drastically season to season. These variables made it difficult to quantify the impact the boom had in terms of an increase in electricity production. In an attempt to do so, the team asked Riki to record data each time he cleaned the inlet of the system. The first data collection occurred from January 23 – 29, 2017. We hoped to use this data as our control and compare it to the data collected after the boom's installation during the week of February 13 – 20, 2017. This data can be seen in Table 4 and Table 5.

Table 4: Pre-boom installation data

Date	Time	Output before cleaning [kW]	Output after cleaning [kW]	Differential [kW]	Yesterday's output [kW]	Notes
Jan 23	7:40 AM	1.20	2.49	1.29	39.0	Dirty water, rain
Jan 24	7:30 AM	2.33	2.49	0.16	52.8	No rain
Jan 25	7:34 AM	2.38	2.50	0.12	57.5	No rain
Jan 26	7:45 AM	2.38	2.51	0.13	57.3	No rain
Jan 27	8:30 AM	2.39	2.51	0.12	57.6	No rain
Jan 28	7:45 AM	2.31	2.46	0.15	57.7	No rain
Jan 29	7:50 AM	2.36	2.45	0.09	56.8	No rain

Table 5: Post-boom installation data

Date	Time	Output before cleaning [kW]	Output after cleaning [kW]	Differential [kW]	Yesterday's output [kW]	Notes
Feb 13	8:00 AM	2.38	2.43	0.05	57.7	No rain
Feb 14	8:00 AM	2.32	2.48	0.16	56.7	Light rain
Feb 15	8:00 AM	2.38	2.44	0.06	56.5	Light rain
Feb 16	8:00 AM	2.43	2.45	0.02	59.0	Light rain
Feb 17	8:00 AM	1.88	1.71	-0.17	29.4	Overnight rain. Inlet gate put on second hole from top. Still raining. Boom seems fine.
Feb 18	6:30 AM	1.10	0.00	-1.10	24.7	Turned off due to flooding. Boom damage, front foam twisted. Boom secure. No action taken.
Feb 19	7:20 AM	2.51	2.51	0	24.7	No rain
Feb 20	8:00 AM	2.46	2.47	0.01	53.7	Light rain

In addition to keeping this log before and after the boom's installation, debris cleared from the intake gate was collected in buckets in hopes of correlating type and quantity of debris with power output. The contents of these buckets are shown in Table 6 and

Table 7. While we were onsite, we never experienced heavy rains, but they would often come through while we were back in Wellington. Heavy rainfall in the second week of data collection resulted in more debris than normal coming downstream, making these efforts to draw conclusions about the effectiveness of the floating boom futile. Furthermore, this data was collected during the summer, when floating debris is minimal compared to the autumn months, when the boom has proven to be more effective.

Table 6: Pre-boom installation debris collection

Date	Photo	Differential [kW]
Jan 23		1.29
Jan 24		0.16
Jan 25		0.12

Jan 26		0.13
Jan 27		0.12
Jan 28		0.15
Jan 29		0.09

Table 7: Post-boom installation data collection

Date	Photo	Differential [kW]
Feb 13		0.05
Feb 14		0.16
Feb 15		0.06

Feb 16		0.02
Feb 17		-0.17

Unfortunately, no quantitative conclusions about the boom's effectiveness could be drawn from this data, as the amount of debris does not correlate with the differential in output power before and after cleaning. This could also be due to the full system flush that Riki executed when he collected the debris and took the data. While a full flush is good for the system, it further impeded the data collection in hopes of quantifying the boom's effectiveness, directly correlating the change in output power with the amount of debris collected. We also found that the water height of the river is a more significant factor than debris with regard to the amount of power produced by the system.

Fortunately, some observations made by Riki regarding the floating boom's durability during storm conditions best define its effectiveness as a way to mitigate intake congestion of the system. Riki stated in an email to the team that another severe flood had occurred since the final modifications had been made in mid-March, and the boom "proved to be robust" as it weathered the storm well. Riki also noted that since the installation of the boom, less maintenance to the intake was required, which will in turn allow Riki and others to allocate more focus on projects such as the native tree nursery and prospective hydroponic greenhouse. Lastly, Riki estimated that the floating boom provided a slight increase in the system's power output.

These results do not yet account for the effectiveness of the mesh screen that was installed in conjunction with the floating boom. Before the 20-year flood occurred that dislodged the rocks used to anchor the mesh to the riverbed, the mesh screen was preventing virtually all debris from entering the system's intake. Though it was not self-cleaning, temporarily shutting the intake gate to stop flow to the turbines created a back-flushing effect and proved to be an effective way of cleaning the mesh. Because the mesh concept has proven to be successful, Riki has plans to modify the mesh, anchoring it to the riverbed in a more permanent fashion. A metal gate will be wedged and securely fastened behind the mesh in the intake so it will not get washed away by another storm.

4.2 Greenhouse Results

4.2.1 Greenhouse structure

Greenhouse Structure

Our greenhouse structure assumes a design quoted by Redpath for NKNT's initial idea of building a 6 m x 16 m nursery for riparian trees. Since the desired properties of greenhouse structures are similar enough between riparian tree farming and watercress growing, we have based our cost estimate on Redpath's previous quote to NKNT (Estimate for Redpath propagation greenhouse, 2016). The building type for this model incorporates RHS, or rectangular hollow section, framing and an "A" shaped top piece to form a pentagonal cross section (Figure 71). The recommended covering is a Twin-skin long-life UV stabilized Duratough ® clear 180 micron external and a Duratough ® clear 180 micron internal greenhouse. Since Duratough ® is primarily comprised of polyethylene, a double glazed polyethylene greenhouse cover was assumed for air heating calculations. The ventilation design includes a set of 1.1 m wide ventilators having an opening of 0.8 m and allowing for optimal air flow (Figure 72). The end walls consist of high

Figure 71: Propagation greenhouse design from RedPath

Figure 72: Ventilation design (Redpath)

quality aluminum framing and an aluminum track that slides to allow entry into the greenhouse. The design parameters we have suggested and used in our calculations are a post height of 1.8 m, with an additional height of 1.8 m from the top of the RHS region to the peak of the roof and cladding. The latter height is not specified in the original quote. This design should be adequate for our theoretical hydroponic greenhouse.

4.2.1 Air Heating Requirements

Air Heating

For this assessment, annual air heating requirements were estimated using a quasi-steady-state energy balance. Modelling was performed in MathCad and used to simulate heating requirements for 24 time periods at 3 different conditions as discussed in Chapter 3.7. The resulting heating requirements are plotted below. For all iterations of daytime heating, no external heating was required. Incident solar radiation accounts for more than enough heat to compensate for heat losses. Thus, nighttime heat requirements are the primary focus of this section. Heat energy requirements were estimated to maintain optimal growing conditions at night for three sets of conditions as displayed in Figure 73. The three conditions were:

a) still air, average cloud cover consistent with weather data
b) windy air of approximately 28 km/h and no cloud cover
c) still air and no cloud cover

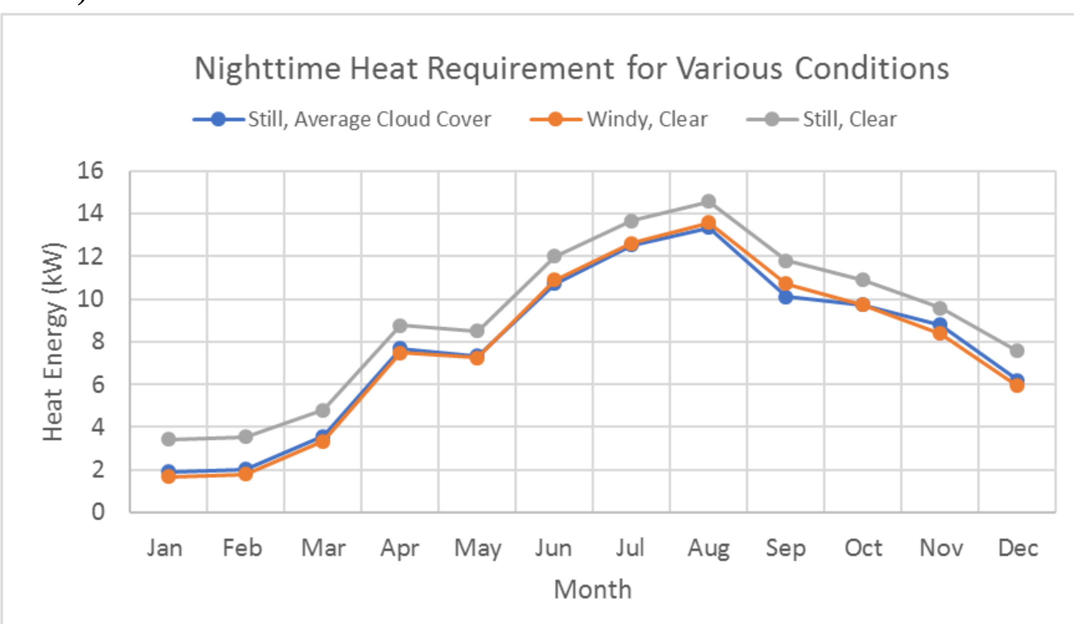

Figure 73: Nighttime Heat Requirement for three Conditions

As shown above, the nighttime heat requirement increases during colder months and decreases during warmer months as expected. The lowest heat requirement estimated was just under 2 kW in January, and the highest requirement of over 14 kW will be required during the month of August, the coldest month in this region of New Zealand. For each set of conditions, the maximum difference per month is approximately 1-2 kW as shown above for still, clear nights compared to windy, clear nights and still nights having an average cloud cover. This result indicates that radiation heat loss is a significant contributor to greenhouse heat losses, but the radiation heat loss is a smaller contributor to the overall heat requirement than the average external temperature.

Wind speed also seems to have a significant effect on heat requirement for the wind speed of 28 km/h tested. Comparing the conditions for b) and c) yields a difference of roughly 1-2 kW per month, which is similar to the difference between clear cloud conditions and average cloud conditions. Interestingly, under the conditions tested, as wind speed increases the overall heat requirement decreases, which may seem counterintuitive. This is a result of convective warming of the outer cover. Since radiation heat loss to the sky lowers the outer cover temperature to below ambient temperature, an increase in wind speed increases convection, resulting in an outer cover temperature closer to ambient. Thus, the total heat requirement is decreased. One might argue that for a given greenhouse design heat loss by infiltration would increase with higher wind speeds. While this is true, the quasi-steady-state model utilized holds the number of air changes per hour constant per the recommendation of Silveston et al. Thus, ventilation remains constant and wind speed only affects the convection coefficient affecting the outer cover temperature. Based on this data, average external temperature appears to dictate heating requirements more than wind speed and cloud cover.

Using our simulated data, which outputs heating values in kW for a given set of conditions, we were also able to estimate annual heating values by averaging a given wattage over the time period. Thus, for a given set of nighttime conditions during a month, the resulting wattage was multiplied by the number of seconds that the heater runs during the month assuming a 12 hour heating period during night. Based on our analysis, nighttime annual heating requirements over the course of a year result in an annual energy requirement of 123-144 GJ/yr, depending on the conditions.

These values do seem reasonable for this size greenhouse when compared with data provided in Pieters & Deltour, 1997, who estimated heating requirements for greenhouses of several cladding materials for growing tomatoes in Belgium. Pieters & Deltour calculated a heat requirement of 1.89 GJ/m^2 of a single layer polyethylene covering including daytime and nighttime heating. Multiplying this value by the cover of our model greenhouse, 205.2 square meters, results in a heating estimate of 387.8 GJ in a year. Our simulation modeled a double layer of polyethylene and only nighttime heating. Combined with the fact that Belgium's climate is colder than New Zealand, our value of less than half of the heating requirement for a Belgian greenhouse seems reasonable. Further, Silveston et al. reported an estimate of 538 GJ/yr for a greenhouse with similar dimensions but 8 meters longer for a single glazed greenhouse in a colder Canadian environment. Thus, our estimates do seem reasonable for maintaining optimum growing conditions for a hydroponic greenhouse in Horohoro, NZ.

Limitations of the Model

For any modelling software or programs, there are limitations that result in error to some degree, the degree of which cannot be quantified unless it is verified empirically. While we minimized potential sources of error, it is impractical for all sources to be fully minimized given the scope and nature of this project. For this model, many parameters used were averages for a given amount of time, including average monthly values for weather data, evapotranspiration rates, and incident radiation rates among others. However, these values came from reputable sources and resulting values should be reasonably close to reality. Further, assuming a quasi-steady-state model results in additional error since many transient inputs are assumed to be constant and the resulting output heat requirement is assumed constant throughout the time period in which the inputs were assumed (i.e. 12 hour nights over the course of a month) in estimations of total energy usage. Although a full model validation was outside the scope of this project, resulting heat requirements seem reasonable compared to other studies as discussed. Despite these challenges, the resulting data should be adequate for generating estimates for this initial feasibility assessment.

Practical Application to the Hydroponic Greenhouse

Once the heating requirement was estimated, a method for providing the heat must be selected. Two methods appear to be most feasible for our project site, geothermal heating or an electrical heat pump. For geothermal heating, our team consulted with Eugene Berrmyan-Kamp from Ngāti Kea Ngāti Tuara to determine if any testing of the ground temperatures had been completed in the area. Eugene recalled that the water temperature was roughly 100°C. A basic layout of a geothermal heating unit is shown in Figure 74.

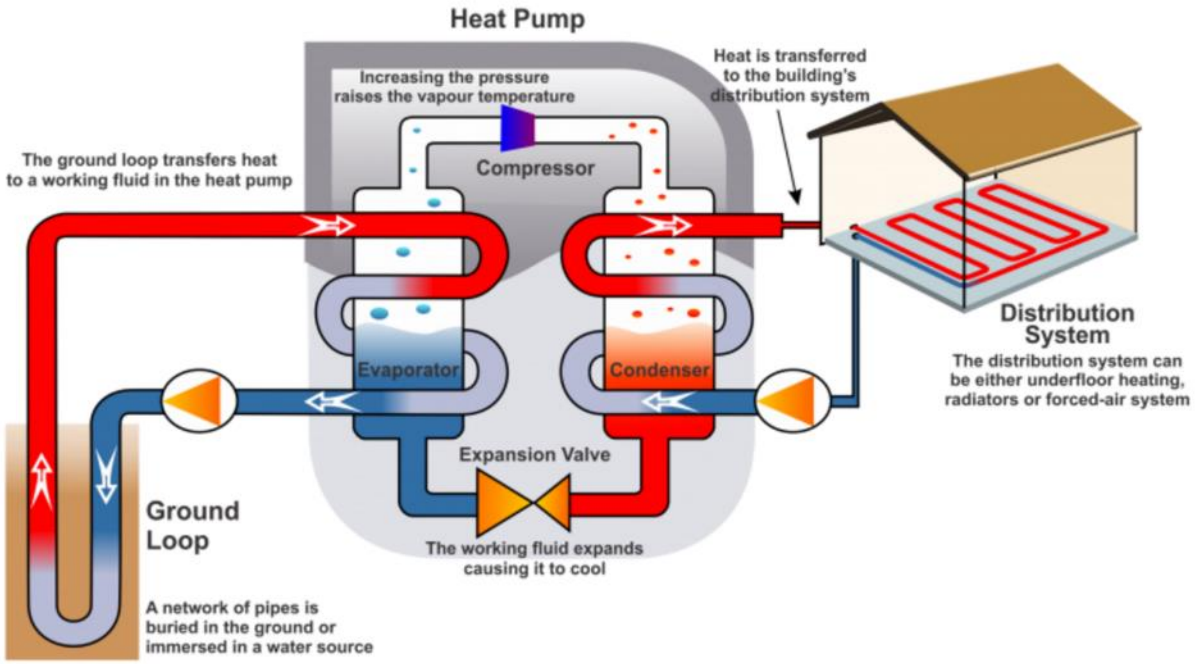

Figure 74: Geothermal heating loop consisting of a ground loop, heat pump, and distribution system. (Williams, 2016)

In this basic layout, initial heat transfer occurs from the geothermal medium underground to the fluid in a pipe. This heated fluid is then circulated through a heat pump where heat is transferred to the working fluid in a heat pump. Heat from the pump is then transferred into a distribution system that would be present in the hydroponic greenhouse.

While this design would be the most sustainable and utilize the geothermal resources present, it has a very high initial cost. While we did not obtain a quote on the price of a full system, Eugene informed us that the cost of tapping into the geothermal land would be approximately $150,000 - $200,000. Given design challenges and the very high initial cost, we geared our design toward a standard heat pump.

Since a key goal of the project is to utilize excess electricity produced by the micro-hydro unit, we researched standard electric heat pumps rather than propane or natural gas pumps. We developed a couple of electric heater designs that are sized to heat the greenhouse under the worst case conditions. We have sized the heater based on a requirement of 18 kW-hours, which allows for a 20% design buffer based on our maximum heating requirement of 14.6 kW during still, clear August nights. We recommend using a unit such as the PUMY-P YKM-A(-BS) Mitsubishi Electric unit seen in Figure 75, sized for 14.0-18.0 kW for effective greenhouse heating. An image of this heat exchanger is pictured to the left.

Figure 75: S Series Mitsubishi Electric heater ("S-Series," 2017)

4.2.2 NFT System Requirements

As described previously, our team selected an NFT system for the hydroponic greenhouse. NFT requires a nutrient solution to be continually circulated in pumps to a series of gullies or set of tables. We selected a design that incorporates gullies, specifically 25 gullies that are 100 mm wide and 100 mm apart to span across the 6 meter wide greenhouse.

Nutrient Solution Tank

For a system of this size, Neville recommends using a tank of roughly 450 L or about 120 gallons. This tank will provide more than enough water for constant recirculation and is also large enough such that sodium concentrations remain low enough to keep the frequency of purging low. Once sodium concentrations rise above a threshold level, the watercress would be negatively affected.

With any nutrient solution, the storage tank must be purged at some frequency, and the waste water must be disposed of properly. While the exact purge frequency necessary to maintain the appropriate nutrient solution concentrations can be based on nutrient monitoring, a general heuristic estimate of 1/3 tank volume per week can be applied according to Neville. Assuming this heuristic holds true, Ngāti Kea Ngāti Tuara would need to replace approximately 40 gallons or 150 L of nutrient solution per week. The waste solution can be dumped onto local farmland since nutrients in the hydroponic solution promote growth of grass in fields (Stocker, 2017). The total water demand is thus 150 L per week, or 7,800 L annually. This amount should be feasible for Ngāti Kea Ngāti Tuara to take from their purified water system located at the marae. However, additional water testing will need to be completed to ensure that the water is suitable for hydroponic watercress production. Watercress is very sensitive to trace levels of some elements. If the marae water is not suitable for hydroponic greenhouse use, a reverse osmosis system or similar unit will need to be installed.

Tank Heat Exchanger Sizing

While air temperature is a vital growing parameter and air heating is beneficial during cold months, nutrient solution temperature is equally important if not more according to Neville. The nutrient solution must be maintained in a specific temperature range to allow for adequate nutrient uptake by plant roots. For watercress, a nutrient solution temperature of 14-18 degrees Celsius must be maintained. Since heat is constantly lost from the nutrient solution tank through the tank walls and from water flowing down the growing tables or gullies, there is significant heat loss to the environment. However, since the system will be indoors, air heating would eliminate the need for nutrient solution heating, but may also introduce the need for cooling.

As discussed previously, air heating is often more costly than it's worth, so we have sized a nutrient solution tank heat exchanger under the assumption that the greenhouse is not heated. We have chosen the ambient temperature to be held constant at 10 degrees Celsius, the coldest average minimum temperature, in order to design the exchanger for the worst case temperature. For this calculation, a polyethylene storage tank manufactured by McMaster Carr was used. Under these assumptions, the heat exchanger was found to require about 6 kW. This unit will also be able to provide cooling if the greenhouse is heated or reaches high temperatures on warm summer days.

Nutrient Solution Pump Sizing

To size the pump, Bright Agrotech recommends sizing based on a pump curve (Figure 76) provided by hydroponic pump supplier Active Aqua. The total flow and head must be known to use the sizing chart. Following the recommendation of University Upstart Farmers (Storey, 2016), we have assumed a flow of 4-6 GPH per trough, resulting in a maximum of 150 GPH needed total. Considering a distance of 15 meters at a 3% incline, we calculated a 0.45 meter drop along the gullies. Adding in a 0.55 meter buffer for the water height in the tank, we estimate that one meter of head will suffice. Thus, we initially sized the pump under the assumption of 1 meter and a 150 GPH water requirement using the chart pictured below, which results in the smallest pump available from the company. However, given an engineering design factor of 15-30% error as Upstart Farmers suggests, we have selected a pump one size up, the AAPW250.

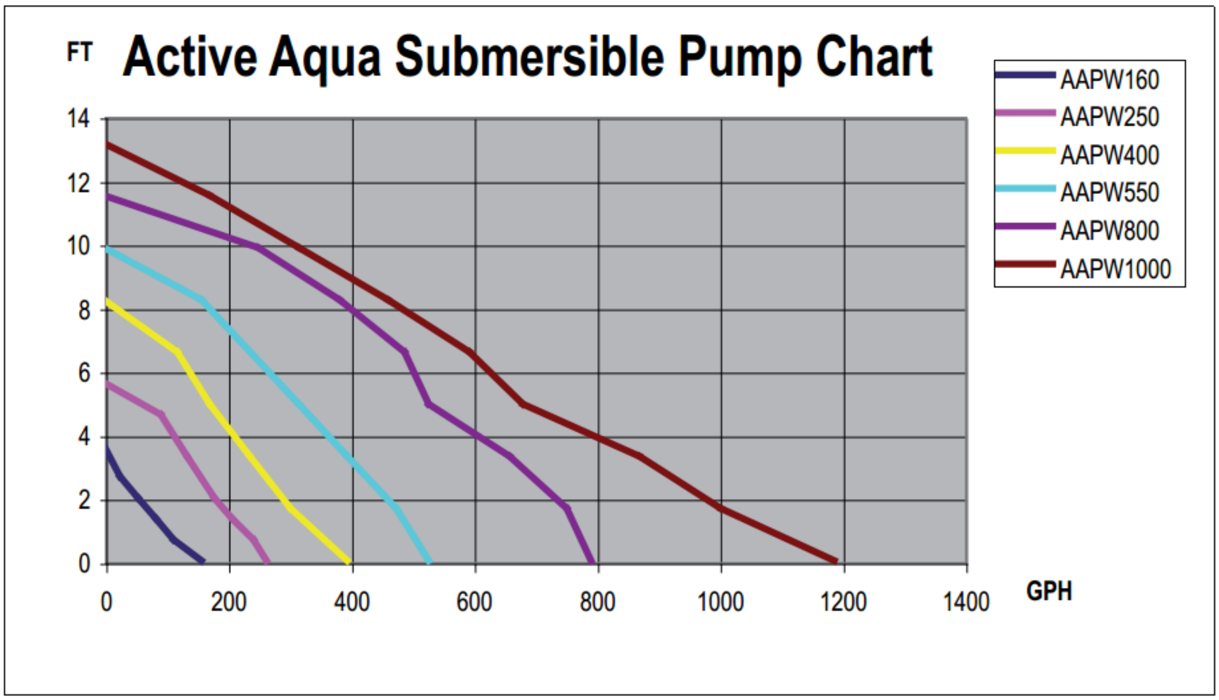

Figure 76: Active Aqua submersible pump chart for sizing hydroponic watering pumps

4.2.3 Electricity Requirements

Ideally, this theoretical hydroponic greenhouse would run solely on the micro-hydro unit's energy. In this section, we attempt to estimate the total amount of electricity required for the greenhouse by each individual electrical component and try to determine if it can be powered by the micro-hydro unit.

Air Heating

If NKNT decides to purchase a heat pump, we recommend heating at night for the six coldest months, May to October. Assuming the heat pump uses approximately 4.47 kW when running, the total power requirement is around 9,762 kWh annually for six months of heating at night.

NFT Hydroponic System

There are several electronic elements of the NFT hydroponic system: the nutrient solution pump, the nutrient solution heat exchanger, automatic dosing system, and thermostat for nutrient solution temperature control.

The nutrient solution pump sized for this system is very small as a result of the low flow rate and head. Our brief calculation estimated an output of only 6-7 watts. While this power requirement seems very small, the manufacturer specifications of the pump from Active Aqua says the selected pump requires only 16 Watts of energy. Assuming this pump is constantly running all year, the total energy requirement for the pump is 504 MJ, or 140 kWh annually based on a 16 W requirement.

Based on our estimates, the nutrient solution heat exchanger will need to output 6 kW of heat for an ambient temperature of 10 degrees Celsius to maintain the appropriate solution temperature. The solution will also likely require cooling during summer months, when temperatures within the greenhouse will escalate. Pure Hydroponics of New Zealand offers nutrient solution heater/chillers that offer 5 times the heating or cooling performance per kW of electrical input. A 2 kW heater/chiller from Pure Hydroponics would maintain an ideal solution temperature in the greenhouse throughout the year with buffer room to spare based on the COP of approximately 5. We estimate that the total energy requirement for the heat exchanger will be approximately 4,370 kWh annually, given that it will run a quarter of the year (summer days and winter nights) at a power requirement of 2 kW.

Automatic dosing control is highly recommended by both Neville Stocker and Paul Mes from Pure Hydroponics NZ. Pure Hydroponics recommends the Bluelab Pro Controller, which probes and controls pH, conductivity, and temperature, the three main parameters closely measured in hydroponic nutrient solutions. They provide exact measurements and automatically deliver the appropriate amounts of nutrient or to the system and will adapt with plant feeding. The system can also be connected to the heating or cooling system. Based on our study, we recommend using this controller to minimize maintenance and likelihood of error. The electronic controlling system requires 5 watts of apparent power according to the user manual provided on the Pure Hydroponics website. Since the system requires 5 watts of energy and would be operating constantly all year, we estimate the total energy requirement to be 158 MJ, or 43.8 kWh annually.

Comparison to Turbine Unit Output

Based on the calculations above, the maximum power requirement for the equipment discussed will be approximately 6.5 kW, the majority of which is drawn from the air heating system sized to use 4.47 kW to heat in cold months at night. Since the current output of the micro hydro unit is approximately 2.40 kW, and an upgraded system with three additional turbines would be just under 5 kW, NKNT would need to draw the additional ~1.5 kW from their electricity suppliers during cold winter nights when electricity requirements are highest even with an upgraded system. However, during warm months when air heating is unnecessary, the current micro hydro unit output would power almost all of the greenhouse, and an upgraded system would certainly power the greenhouse based on our estimations. It is important to note that power use of the turbine fluctuates season to season depending on events at the marae and heat use, but typically between half and three quarters of the energy produced by the turbines is sold back to the electricity suppliers based on NKNT electric bills from the past year. Thus, assuming 1.2-1.8 kW of energy is available from the current system, approximately 0.3 – 1.0 kW of supplemental power from the grid would likely be necessary with the air heating off, but no additional power would be required if the turbine unit was upgraded.

With the addition of three turbines to the micro hydro unit, the output could be increased to approximately 3.6-4.2 kW, assuming the additional turbines output 2.4 kW as the current turbines do. During the six months that air heating took place at night, the air heating power requirement would be reduced to 589 kWh - 1,900 kWh, and the total requirement would be 681 kWh – 1,992 kWh assuming the heater/chiller was not turned on. During the remaining six months, the total power requirement would be fully covered by the turbine unit.

4.2.4 Cost Estimate

Air Heating

According to NKNT's December 2016 energy bill at the marae, the cost of electricity from the grid is 21.6 cents per kWh. For 9,762 kWh of energy used to heat the greenhouse without aid from the micro hydro unit, it would cost approximately NZ$2,109 annually to heat the greenhouse assuming nighttime heating during the coldest 6 months of the year. Assuming 3.6 kW to 4.2 kW of energy was available from an upgraded turbine system during this time, the total cost of heating would be approximately NZ$127 - $410 annually for 589 kWh - 1,900 kWh of energy. A heat pump system of this size would cost approximately NZ$8,000 – 10,000 according to Steve Turner of Temprite Industries (NZ) Ltd.

NFT Hydroponic System

Based on the nutrient solution pump's annual electricity requirement of 140 kWh, the total cost to run the inline pump will be NZ$30.26 annually if energy is purchased from the grid. This is a fairly low energy cost, but the total circulation requirement is equally low. The estimated cost of the pump from Bright Agrotech online is NZ$37.01 for the initial purchase. A similar size pump from Stocker Horticulture & Hydroponic Supplies LTD in New Zealand costs NZ$38.00.

According to our estimation for the heat exchanger annual electricity requirement, the total grid energy cost to heat the nutrient solution will be approximately NZ$943.50 annually for operation during hot summer days and cold winter nights. The estimated cost of the heat exchange system is about NZ$5,000. It is important to note that this estimate for electricity usage by the nutrient solution heater/chiller was based on the assumption of no air heating in the greenhouse. The 130 gallon McMaster-Carr tank used for calculations is approximately NZ$700.

Lastly, the automatic dosing Bluelab Pro Controller system will utilize 43.8 kWh annually, resulting in an annual electricity cost of NZ$9.46. The retail price of the system according to Pure Hydroponics is NZ$2,980.

According to Paul Mes from Pure Hydroponics, the cost of an NFT hydroponic system setup, including piping and plant work is approximately NZ$68 per square meter for a given greenhouse, which excludes storage tanks, greenhouse structure, and heating systems. Thus, for a 6 x 16 greenhouse incorporating gullies spaced 100 mm apart, an approximation for the setup would be NZ$6,528. Thus, an initial approximation for an NFT Hydroponic System of this size is approximately NZ$15,000.

Greenhouse Structure

Our greenhouse structure assumes a design quoted by Redpath for NKNT's initial idea of building a 6 m x 16 m nursery for riparian trees. The total price for the greenhouse materials was quoted at NZ$9,955.00. with construction adding an additional NZ$9,780. Thus, the total greenhouse structure cost will be approximately NZ$19,735.

Total Cost

Summing together the costs of the air heat pump, hydroponic nutrient solution pump, solution storage tank, heat exchanger, piping/planting, and greenhouse construction, we estimate the total cost to be approximately NZ$45,000 - NZ$50,000 for the first year depending on energy use. If the turbine system is to be upgraded, this cost will rise to NZ$80,000 - NZ$85,000 per estimates from NKNT. Approximately NZ$10,000 is attributed to greenhouse heating, NZ$15,000 for hydroponic system installation, NZ$20,000 for greenhouse construction, and NZ$35,000 for turbine system upgrade. The remainder is associated with electricity costs and a roughly 10% buffer. Note that this price estimation does not include any costs associated with labor and project management while the greenhouse is in operation.

Chapter 5: Conclusions and Recommendations

5.1 Floating Boom and Mesh System

As demonstrated in the results section, the floating boom and mesh system successfully deters floating debris and catches submerged debris. Thus, our initial design goal was achieved, and the buoyancy and stability calculations proved to be reasonably accurate. Additionally, the storms and flood conditions have proven to be a good test of the boom's durability, and it has survived. However, they have also given the team insight into areas of improvement. With this knowledge, the team developed recommendations for future work:

1. Consider including a light-weight top piece like the Alden Laboratory model, which would prevent deformation and keep the foam from bowing upwards between the threaded rod. This would require more foam and thus increase the cost. It would also decrease the boom's flexibility, which has proven to be a useful feature, and compromise its stability to some degree, should the NKNT choose this course of action.
2. If option 1 was pursued, the use of thicker foam would be necessary to account for the additional weight and water absorption into the foam.

3. Drill pilings into the river bed so that the boom can rise and fall with or another permanent anchoring system, which would eliminate drag on the ropes and increase longevity.
4. Permanently anchor the mesh to the riverbed instead of by land to prevent the mesh from dislodging during flood conditions. Riki Oneroa plans to wedge a gate into the inlet and press the mesh against it, which would secure the assembly.

We anticipate that the floating boom and mesh screen implemented at the inlet of the micro-hydro unit at Ngāti Kea Ngāti Tuara will continue to lessen the hours spent clearing debris from the intake and ultimately increase electricity production. These recommendations are meant to convey where the boom and mesh might be improved.

5.2 Greenhouse Design

Although air heating in greenhouses is often not necessary given New Zealand's temperate climate, it can significantly boost production during winter months when temperatures drop to around ten degrees Celsius. If funds sufficient funds are available, we recommend heating the air at night during the coldest six months of the year using a heat pump such as the Mitsubishi Electric PUNY-P140YKM-A (-BS) that can output 18.0 kW of heat. However, if cost cuts must be made, we recommend eliminating air heating before sacrificing other equipment.

For the hydroponic system, we strongly recommend using the nutrient film technique for growing watercress per the advice of literature and hydroponic experts. A small hydroponic solution pump will suffice for this size greenhouse and we recommend choosing a pump similar to the AAPW250 or the 1054 Aqua One 103. We also recommend heating the nutrient solution tank with a heat exchanger such as the Pure Hydroponics heater/chiller which can output 6 kW of heat in order to maintain proper nutrient solution temperature stored in a tank such as the polyethylene tank from McMaster-Carr. Lastly, we suggest purchasing the Bluelab Pro Controller auto-dosing system to ensure proper control of the hydroponic system.

Based on our analysis, the total water requirement for this system should be on the order of 7,800 L annually and the total electricity requirement with air heating will be approximately 14,315 kWh annually. With energy from an upgraded micro-hydro system, the amount purchased from the grid would fall to between approximately 681 kWh – 1,992 kWh, since all equipment could be fully powered while the air heat pump is not running. Without air heating, the total electricity requirement will be approximately 4,550 kWh annually. An upgraded micro-hydro system could theoretically supply all of this energy assuming the maximum requirement at any time is under 2.5 kW. The total cost of the greenhouse and its equipment will be approximately NZ$45,000 - $50,000 during the first year, which does not include any costs associated with labor and project management. With an upgrade of the hydroelectric unit, this price will increase to around NZ$80,000 - $85,000.

Based on our calculations, we believe the electricity and water requirements are reasonably attainable at the marae, and a hydroponic greenhouse is feasible assuming funding is approved and marae water quality meets the standard for hydroponic watercress production. Our team recommends further research in a cost-benefit analysis of watercress production before moving forward with the idea as well a more detailed design and quote from a Hydroponics business such as PGO Horticulture LTD.

Works Cited

"6 mil sheeting – 4 year." (n.d.). Rimol Greenhouse Systems. Retrieved from https://store.rimolgreenhouses.com/6_Mil_Sheeting_4_Year_p/ktiv6.htm

A Brief History. (2016). *New Zealand Now*. Retrieved 29 November 2016, from https://www.newzealandnow.govt.nz/living-in-nz/history-government/a-brief-history

Bargh, M. (2012). Rethinking and re-shaping indigenous economies: Māori geothermal energy enterprises. *Journal Of Enterprising Communities: People And Places In The Global Economy*, *6*(3), 271-283. http://dx.doi.org/10.1108/17506201211258423

Bargh, M. (2015). Project Description. Victoria University of Wellington.

Berryman-Kemp, E. (2016). NKNT Strategic Plan. Presentation, Te Runanga o Ngāti Kea Ngāti Tuara.

Cengel, Y. & Ghajar, A. (2015). *Heat and Mass Transfer: Fundamentals & Applications.* New York: New York. McGraw-Hill Education.

"Chapter 1 – Introduction to evapotranspiration." (n.d.) FAO Corporate Document Repository. Retrieved from http://www.fao.org/docrep/x0490e/x0490e04.htm

"Commercial hydroponic growing systems." (2017). Pure Hydroponics. Retrieved from http://purehydroponics.com/commercial-systems/commercial-hydroponic-systems/

"Cross country cottage 12 x 16 glass greenhouse." (n.d.). Greenhouse Nation. Retrieved from https://www.greenhousenation.com/cross-country-cottage-12x16-glass-greenhouse-p-595.html

Daigneault, A., Eppink, F., & Lee, W. (2017). A national riparian restoration programme in New Zealand: Is it value for money? Journal Of Enviromental Mangement. 187, 166-177.

Datko, S. "How to grow hydroponically – overview of grow systems." (2012). San Diego Hydroponics. Retrieved from http://sdhydroponics.com/2012/05/11/how-to-grow-hydroponically-overview-of-grow-systems/

Davis, Scott. Serious Microhydro : Water Power Solutions from the Experts. New York, US: New Society Publishers, 2010. ProQuest ebrary. Web. 17 November 2016.

"Deep water culture hydroponics system." (n.d.). The Moore Mark. Retrieved from http://themoormart.com/product/deep-water-culture-hydroponic-system/

“Ebb and flow hydroponic systems.” (n.d.) Gardenious. Retrieved from http://gardenious.com/tag/ebb-and-flow-hydroponic-system-design/

Floating Marine Trash and Debris | Containment Boom | Elastec. *Elastec*. Retrieved 25 January 2017, from https://www.elastec.com/products/floating-boom-barriers/trash-debris-boom/

George, K. (2016). *Ngāti Kea Ngāti Tuara Iwi Environmental Management Plan 2016* (p. 14). Rotorua, NZ.

Gonzalez et. al. (2016). Integrative conservation of riparian zones. Biological Conservation.

Google Maps. (2017). Floating Boom Intake at the Indiana-Kentucky Electric Corporation. Retrieved from https://www.google.co.nz/maps/place/Madison,+IN,+USA/@38.7360699,-85.4207347,338m/data=!3m1!1e3!4m5!3m4!1s0x886a3ae6e352496b:0x9bce9b78b2c9ef3a!8m2!3d38.7358933!4d-85.3799577

“Greenhouse construction, types, or style information guide.” (2006). EnviroCept. Retrieved from http://www.envirocept.com/gh_guide/greenhouse_kits.html

“Greenhouse products – fiberglass conversion kit for Biltmore greenhouses.” (n.d.) Turner Greenhouses. Retrieved from http://turnergreenhouses.com/product/fiberglass-conversion-kit-for-biltmore-greenhouses/

History | Ngāti Kea Ngāti Tuara. (2016). Ngatikeangatituara.com. Retrieved 29 November 2016, from http://ngatikeangatituara.com/history/

“Hydro/Aquaponics.” (2016). Hawaiian Hydro & Garden. Retrieved from http://www.hawaiianhydroandgarden.com/hydroaquaponics/

“Hydroponic Drip System.” (n.d.). Home Hydro Systems. Retrieved from http://www.homehydrosystems.com/hydroponic-systems/drip_systems.html

“Hydroponics.” (2015). Mission 2015: Biodiversity. Retrieved from http://web.mit.edu/12.000/www/m2015/2015/hydro_agriculture.html

“Hydroponic Systems 101: Learn the basics of hydroponics.” (n.d.) Full Bloom Hydroponics. Retrieved from http://www.fullbloomhydroponics.net/hydroponic-systems-101/

Kimura, K. & Stephenson, D. G. (1969). “Solar Radiation on Cloudy Days.” National Research Council of Canada. Retrieved from http://web.mit.edu/parmstr/Public/NRCan/rp418.pdf

Land Use Environmental Snapshot. (2010). Ministry for the Environment. Retrieved 29 November 2016, from http://www.mfe.govt.nz/more/environmental-reporting/reporting-act/land/land-use-indicator/land-use-environmental-snapshot.

Mashonjowa et. al. (2013). Modelling the thermal performance of a naturally ventilated greenhouse in Zimbabwe using a dynamic greenhouse climate model. Solar Energy. 91, 381-393.

“Metacentric height.” (n.d.). Mechanical Engineering Community. Retrieved from https://mechanical-engg.com/gallery/image/1953-metacentric-height-please-explainjpg

“N.F.T. (nutrient film technique) System.” (n.d.). Home Hydro Systems. Retrieved from http://www.homehydrosystems.com/hydroponic-systems/nft_systems.html

“Nutrient film technique – NFT Hydroponics.” (2017). No Soil Solutions. Retreived from http://www.nosoilsolutions.com/tag/nft/

“Nutrient Solution Heater/Chillers.” (n.d.) Pure Hydroponics. Retrieved from http://purehydroponics.com/products/lighting-heating/nutrient-solution-heaterchillers-2/

Ostermeier, J. (2008). *Microhydro Intake Design | Home Power Magazine*. *Homepower.com*. Retrieved 25 November 2016, from https://www.homepower.com/articles/microhydro-power/design-installation/microhydro-intake-design

“Our technology.” (n.d.) AeroFarms. Retreived from http://aerofarms.com/technology/

Pieters, J. G., and J. M. Deltour. "Performances of greenhouses with the presence of condensation on cladding materials." Journal of Agricultural Engineering Research 68.2 (1997): 125-137.

PowerSpout LH Case Study: Installation at Kearoa Marae In association with Te Runanga o Ngāti Kea Ngāti Tuara. (2014) (1st ed.). Retrieved from http://www.powerspout.com/assets/Published/public/LH/LH-Installs/LH-case-study-april-2014-published.pdf

Purpose. (2016). The Waikato River Authority. Retrieved 29 November 2016, from http://www.waikatoriver.org.nz/about-the-waikato-river-authority/purpose/

Royal, C. (2007). Kaitiakitanga – guardianship and conservation – Te Ara Encyclopedia of New Zealand. Teara.govt.nz. Retrieved 29 November 2016, from http://www.teara.govt.nz/en/kaitiakitanga-guardianship-and-conservation

"S-Series: PUMY." (2017). Mitsubishi Electric NZ. Retrieved from http://www.mitsubishi-electric.co.nz/citymulti/c/7840/s-series-pumy

Silveston, P. L., et al. "Energy conservation through control of greenhouse humidity. I. Condensation heat losses." Canadian Agricultural Engineering 22.2 (1980): 125-132.

Singh, S. (2012). *Experiments in fluid mechanics* (p. 12). Prentice-Hall Of India Pv.

Storey, A. (2016) "Sizing a pump for hydroponics or aquapoints." University Upstart Farmers. Retrieved from https://university.upstartfarmers.com/blog/sizing-a-pump-for-hydroponics-or-aquaponics

"The advantages and disadvantages of 4 major hydroponic growing systems." (2011). Easy Hydroponics. Retrieved from http://www.easyhydroponics.net/the-advantages-and-disadvantages-of-4-major-hydroponic-growing-systems.html.

"The quality plus." U.S. Global Resources. Retrieved from http://www.usgr.com/greenhouses/quality-plus.php

"Thermal Conductivity of common Materials and Gases." (n.d.) The Engineering Toolbox. Retrieved from http://www.engineeringtoolbox.com/thermal-conductivity-d_429.html

Waitangi Tribunal. (2016). Treaty2u.govt.nz. Retrieved 29 November 2016, from http://www.treaty2u.govt.nz/the-treaty-today/waitangi-tribunal/

"What is hydroponics?" (2008). Simply Hydroponics. Retrieved from http://www.simplyhydro.com/whatis.htm.

"Wick growing system." (n.d.) Hanna Instruments. Retrieved from http://hannainst.com/hydroponics-wick-growing-system

"Wick system." (n.d.) Home Hydro Systems. Retrieved from http://www.homehydrosystems.com/hydroponic-systems/wick-system_systems.html

Williams, H. (2016). "Geothermal heat pumps." Geothermal Heat Pump Association of New Zealand. Retrieved from http://nzgeothermal.org.nz/ghanz/geothermal-heat-pumps/

Chapter 6: Appendices

6.1 News Articles and Publicity of Micro-hydro Project

Project Whenua, Series 1 Episode 10

Tuesday 16 December 2014

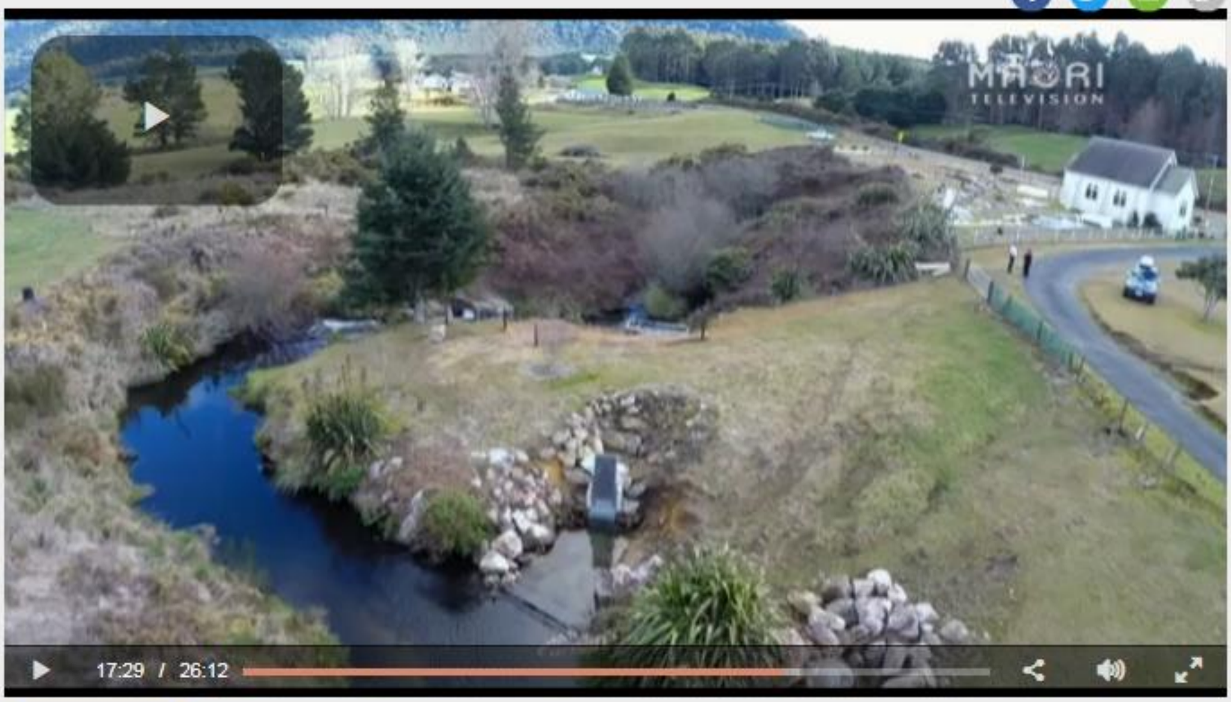

Add to...

Hands-on science series. By installing a micro-hydro unit on the Pokaitu stream, Ngāti Kea Ngāti Tuara are now generating their own power. We find out about their future plans for self-sufficiency.

Link: http://www.maoritelevision.com/tv/shows/project-whenua/S01E010/project-whenua-series-1-episode-10

ROTORUA Daily Post

Weekender: Hydro unit helps save on marae power bills

By Mike Watson

POWER BROKER: Project manager Eugene Berryman-Kamp beside the micro-hydro unit, which is saving Kearoa Marae.

Eugene Berryman-Kamp is a contented man.

Eugene's marae at Kearoa, south west of Rotorua, has installed a small hydro power unit to generate electricity, saving at least $4000 a year in expensive power bills.

The micro-hydro unit, which has three turbines producing 2.5 kilowatts per hour, will be used to provide power to the marae, nearby iwi-owned trust farm and to grow vegetables in hydroponic glasshouses on the marae land, says Eugene.

Te Runanga o Ngati Kearoa Ngati Tuara came up with the idea of generating their own electricity to cut costs at a hui two years ago, says project manager Eugene.

The Apirana Rd marae buildings were used intermittently for events and functions, such as tangi and hui, resulting in spikes in electricity use.

The iwi decided to harness the nearby Pokaitu Stream behind the marae and divert the water flow through a culvert to three turbines and generate power.

There is capacity to install three more turbines to maximise generation up to 5kw/h - more than the marae presently needs, Eugene says.

Before the hydro was installed the marae was using around 18,000kw of power annually at around 22 cents a kilowatt, he says.

The three turbines can generate about 23,000 kw per year - slightly more than current power consumption for the marae and the associated farm trust, with the excess being sold into the grid.

The turbines are connected to the switchboard in the marae and an import-export meter installed to enable surplus power to be put into the main power grid.

Potaiku Stream, and other nearby waterways, have been historically, spiritually and culturally significant to the iwi for more than 100 years, Eugene says.

A waterwheel was installed on the stream for a flax mill, and the birds, eels and fish were used as food source.

Ngati Kearoa Ngati Tuara is one of three iwi involved in the Te Arawa River Iwi Trust assigned to help restore the Waikato River, he says.

The trust is involved in sustainable use of natural resources which fits well with the idea of installing a hydro power unit, Eugene says.

"It's not a complicated process to generate our own electricity and become independent of the national grid.

"We wanted to achieve sustainable energy generation with minimal environmental impact," he says.

Across the stream the iwi have fenced off riparian land and replanted 1000 native trees.

"If we want to be self-sustaining we have learnt you can't shake your finger at others unless you clean up your own backyard first."

For more info contact Eugene at nkntgm@xtra.co.nz.

Link: http://www.nzherald.co.nz/rotorua-daily-post/news/article.cfm?c_id=1503438&objectid=11228119

Marae makes history by generating own power

Editor's Pick   Indigenous   Lastest News   Whanau, Hapu, Iwi, Marae   Aug 13, 2015

Because of escalating power costs, Te Runanga o Ngāti Kearoa Ngati Tuara has turned to harnessing power from a river behind their marae just out of Rotorua, to generate their own power.

A dream that started in 2012 has become a reality for Ngati Kearoa Ngati Tuara descendents. Their marae at Kearoa, south west of Rotorua has become the first in Aotearoa New Zealand to generate their own power.

The micro-hydro unit, which has three turbines producing 2.5 kilowatts per hour, will be used to provide power to the marae, nearby iwi-owned trust farm and to grow vegetables in hydroponic glasshouses on the marae land, explained project manager Eugene Berryman-Kemp to Rotorua's Weekender.

The unit has been so effective it has saved over $4000 a year in power bills. The three turbines can produce roughly 23,000 kw per year – this equates to slightly more than the marae's current power consumption as well as the associated farm trust, with the excess being sold into the grid.

Potaiku Stream, and other nearby waterways, have been historically, spiritually and culturally significant to the iwi for more than 100 years, Eugene says.

Ngati Kearoa Ngati Tuara is one of three iwi involved in the Te Arawa River Iwi Trust assigned to help restore the Waikato River, he says.

- For more info contact Eugene at nkntgm@xtra.co.nz.

Additional reporting by Weekender journalist Mike Watson

Link: http://news.tangatawhenua.com/2015/08/34490/

Link: http://energynzmag.co.nz/innovations/micro-hydro-projects-gain-in-popularity/

(http://energynzmag.co.nz/)

Home (http://energynzmag.co.nz/) / Innovations (http://energynzmag.co.nz/category/innovations/)

Micro hydro projects gain in popularity

OCTOBER 22ND, 2015 ENERGYNZ MAGAZINE (HTTP://ENERGYNZMAG.CO.NZ/AUTHOR/ENERGYNZMAG/)

INNOVATIONS (HTTP://ENERGYNZMAG.CO.NZ/CATEGORY/INNOVATIONS/)

In the face of escalating power costs rural Maori settlements are turning to generation of their own power from local resources.

NGATI KEAROA NGATI TUARA, one of three Te Arawa sub tribes in Te Arawa River Iwi Trust, has completed a micro-hydro project at its marae at Kearoa, south west of Rotorua (becoming the first marae to generate its own power).

The idea emerged at a renewable energy hui at Kearoa Marae in 2011 and a feasibility study identified the nearby Pokaitu Stream as suitable for a micro-hydro unit. At the turn of last century, the stream site had been used to power a waterwheel for a flax mill.

(https://i2.wp.com/energynzmag.co.nz/wp-content/uploads/2015/11/Energy-Magazine-Te-Arawa-River-Iwi-Trust-Content-Image-1.jpg)

Te Arawa River Iwi Trust Content Image

A 600mm pipe conveys the water to the headstock where the turbines are located. The headstock is designed to hold six turbines, but only three have been installed so far. A flow rate of approximately 50 litres per second is required for each turbine, so the maximum requirement for the system is 300 litres per second. This is less than half of the summer low flow (700 litres per second).

The water drives the propeller turbines as it falls around three metres back to the river via draft tubes. The water returning to the river falls on solid rock, which prevents erosion.

It was estimated that each turbine should generate 700 to 800 kilowatts. The three turbines produce 2.5 kilowatts per hour, powering the marae and a nearby iwi-owned trust farm that grows vegetables in hydroponic glasshouses. Excess power is sold into the grid.

Project manager Eugene Berryman-Kemp says the unit has been so effective it has saved over $4000 in power costs over the past year.

Related

A HUGE SCHEME AND A LONG BUILD (http://energynzmag.co.nz/hydro/a-h scheme-and-a-long-build/)
June 12, 2013
In "Hydro"

The power of 3 (http://energynzmag.co.nz/geotherm power-of-3/)
March 15, 2012
In "Geothermal"

Looking off-shore (http://energynzmag.co.nz/generatio off-shore/)
January 25, 2015
In "Features"

TAGS **KEAROA MARAE (HTTP://ENERGYNZMAG.CO.NZ/TAG/KEAROA-MARAE/)**

TE ARAWA RIVER IWI TRUST (HTTP://ENERGYNZMAG.CO.NZ/TAG/TE-ARAWA-RIVER-IWI-TRUST/)

6.2 Pokaitu Stream Information

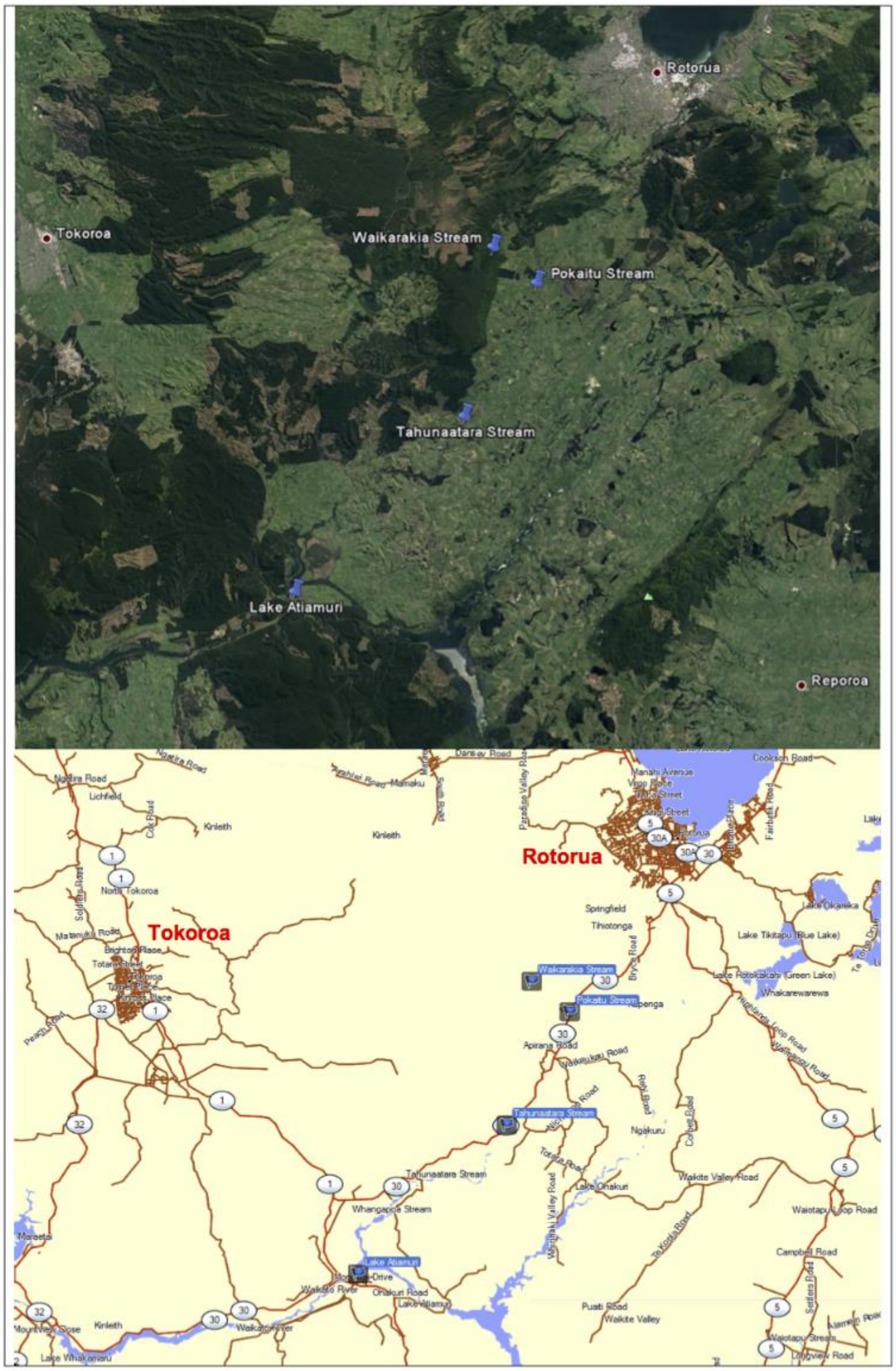

Site 1		Hydrol Number	3157.1
River/Stream	Waikarakia	Tideda Number	-
Site Name	Downstream from spring	Google Map GPS ref	S38 13.281,E176 08.949
Region	Bay of Plenty	Map Reference	BF36 757 649

Landowner Contact		Latest update	11/01/2017	Updated description by	Trent Stokes

Pace Notes

Head south from Hamilton via SH1. Take the first exit onto SH5 at the roundabout past Tirau towards Rotorua. Continue through Rotorua on SH5, before turning right onto SH30 at Hemo Rd. After 1 km continue onto SH30 by turning right. After 10 km turn right onto Apirana Rd. Travel 4 km down Apirana (turns into Kearoa Rd) and park next to a gate leading to a stock yard.

Location Description/Comments

Climb over the fence, head down short race to the left of the stockyard. At the end of the race follow fence line that separates the two paddocks (see photo). Cross the stream and follow the farm track until the style leading to the bush is visible. Follow the pink markers for approximately 500 m until the stream reach (see photo) is visible.

Hazards

Slip/Trip – Climbing fences, walking through bush and uneven ground.
Bulls may be present.

Approx Time (guide for OSH call in)	-

Location Map

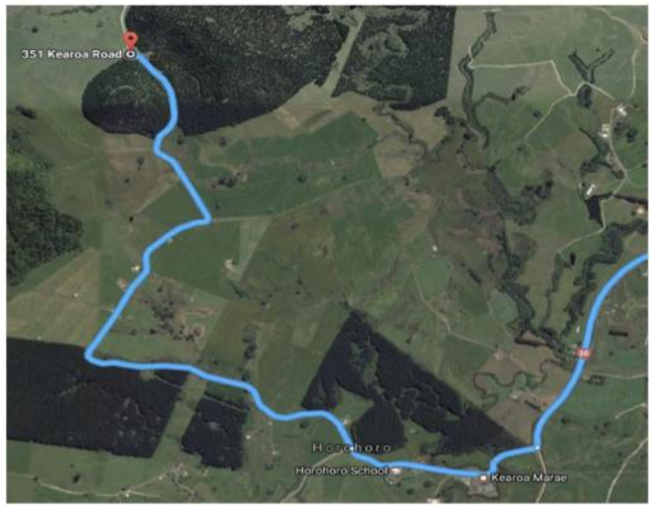

Site 2		Hydrol Number	3158.1
River/Stream	Pokaitu	Tideda Number	-
Site Name	Kearoa Marae	Google Map GPS ref	S38 14.334,E176 10.570
Region	Bay of Plenty	Map Reference	BF37 780 629

Landowner Contact		Latest update	11/01/2017	Updated description by	Trent Stokes

Pace Notes

Head back down Kearoa/Apirana Rd towards SH30. The Marae is approximately 400 m on the right before reaching SH30, can be spotted on the way to site 1.

Location Description/Comments

Enter the main gate to the Marae and cut across the grass in front of the buildings. Park by the riparian strip near the swimming hole.

Hazards

Slip/trip – uneven ground heading into sampling area.

Approx Time (guide for OSH call in)

Location Map

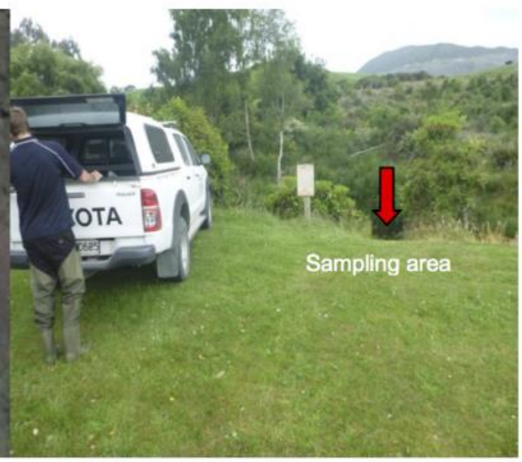

Site 3				Hydrol Number	934.13
River/Stream	Tahunaatara			Tideda Number	-
Site Name	SH30 Bridge			Google Map GPS ref	S38 18.241,E176 07.879
Region	Bay of Plenty			Map Reference	BF36 739 557
Landowner Contact		Latest update	11/01/2017	Updated description by	Trent Stokes

Pace Notes	
Head back to SH30 and turn right. Continue for 9.2 km before arriving at the site located under the road bridge.	
Location Description/Comments	
Turn off SH30 onto a forestry road which veers off to the right where you can park under the bridge.	
Access to water is just downstream from the bridge.	
Hazards	
Slip/trip – access to water is uneven	
Approx Time (guide for OSH call in)	

Location Map

Site 4		Hydrol Number	1854.3
River/Stream	Waikato River	Tideda Number	-
Site Name	Lake Atiamuri Boat ramp	Google Map GPS ref	S38 23.386, E176 01.546
Region	Bay of Plenty	Map Reference	BF36 643 469

Landowner Contact		Latest update	11/01/2017	Updated description by	Trent Stokes

Pace Notes	Location Map
Continue along SH30 down to SH1. Turn left onto SH1 and travel 7.3 km before turning left onto Hanui Rd. At the end of Hanui turn left onto Tia St and follow this road to the boat ramp.	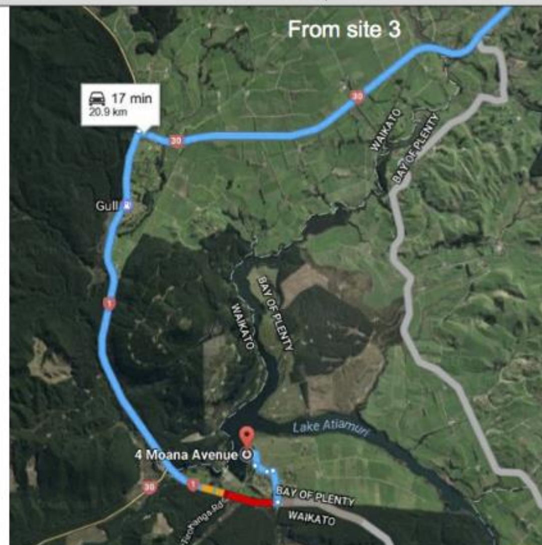
Location Description/Comments	
Sample out from boat ramp.	
Hazards	
Slips/trips – boat ramp and surrounds can be slippery.	
Approx Time (guide for OSH call in): -	

Hill Laboratories
TRIED, TESTED AND TRUSTED

R J Hill Laboratories Limited
1 Clyde Street Hamilton 3216
Private Bag 3205
Hamilton 3240 New Zealand

T 0508 HILL LAB (44 555 22)
T +64 7 858 2000
E mail@hill-labs.co.nz
W www.hill-laboratories.com

ANALYSIS REPORT

Client:	Waikato Regional Council	**Lab No:**	1698086
Contact:	Asaeli Tulagi	**Date Received:**	15-Dec-2016
	C/- Waikato Regional Council	**Date Reported:**	04-Jan-2017
	Private Bag 3038	**Quote No:**	37495
	Waikato Mail Centre	**Order No:**	D1204 4.2
	Hamilton 3240	**Client Reference:**	TARIT
		Submitted By:	Asaeli Tulagi

SPv1

Sample Type: Aqueous

Sample Name:		Waikarakia 15-Dec-2016 9:47 am	Pukaitu 15-Dec-2016 11:01 am	Tahunaatara 15-Dec-2016 11:30 am	Atiamuri 15-Dec-2016 12:40 pm	
Lab Number:		1698086.1	1698086.2	1698086.3	1698086.4	
Absorbance at 340, 440, 780nm						
Absorbance at 340 nm	AU cm^{-1}	0.010	0.015	0.023	0.009	-
Absorbance at 440 nm	AU cm^{-1}	0.002	0.003	0.005	< 0.002	-
Absorbance at 780 nm	AU cm^{-1}	< 0.002	< 0.002	< 0.002	< 0.002	-
Waikato River Run Profile						
Turbidity	NTU	0.73	1.67	2.7	1.71	-
pH	pH Units	7.3	7.2	7.1	7.7	-
Electrical Conductivity (EC)	mS/m	5.6	5.8	7.8	15.7	-
Total Dissolved Solids (TDS)	g/m^3	96	82	108	118	-
Total Arsenic	g/m^3	< 0.0011	< 0.0011	0.0152	0.028	-
Boron	g/m^3	0.007	0.007	0.013	0.28	-
Lithium	g/m^3	0.0042	0.0051	0.0107	0.092	-
Chloride	g/m^3	3.6	3.3	4.5	16.5	-
Total Ammoniacal-N	g/m^3	< 0.010	< 0.010	< 0.010	< 0.010	-
Nitrite-N	g/m^3	< 0.002	< 0.002	< 0.002	< 0.002	-
Nitrate-N	g/m^3	0.163	0.35	0.54	0.066	-
Nitrate-N + Nitrite-N	g/m^3	0.163	0.35	0.54	0.067	-
Total Kjeldahl Nitrogen (TKN)	g/m^3	0.11	0.13	0.19	0.19	-
Dissolved Reactive Phosphorus	g/m^3	0.032 #1	0.024	0.037	0.009	-
Total Phosphorus	g/m^3	0.031 #1	0.029	0.038	0.016	-
Total Biochemical Oxygen Demand ($TBOD_5$)	g O_2/m^3	< 0.8	< 0.8	< 0.8	< 0.8	-
Dissolved Non-Purgeable Organic Carbon (DNPOC)	g/m^3	1.5 #2	1.9 #2	1.6	1.1	-
Non-Purgeable Organic Carbon (NPOC)	g/m^3	1.4 #2	1.5 #2	2.5	1.4	-
Chlorophyll a	g/m^3	< 0.003	< 0.003	< 0.003	0.005	-
Waikato River Run Profile Extra Testing 2016						
Sum of Anions	meq/L	0.52	0.54	0.73	1.43	-
Sum of Cations	meq/L	0.51	0.55	0.75	1.49	-
Total Alkalinity	g/m^3 as $CaCO_3$	18.5	19.4	26	40	-
Bicarbonate	g/m^3 at 25°C	23	24	31	49	-
Dissolved Calcium	g/m^3	1.44	1.87	2.7	6.3	-
Dissolved Magnesium	g/m^3	0.64	0.85	1.30	2.6	-
Dissolved Potassium	g/m^3	3.0	2.6	3.1	2.9	-
Dissolved Sodium	g/m^3	7.0	7.5	9.9	20	-
Reactive Silica	g/m^3 as SiO_2	68	59	64	35	-
Sulphate	g/m^3	1.6	1.4	2.1	7.3	-

Analyst's Comments

Due to workload pressure, we were unable to commence the TBOD on the day that they arrived at the laboratory. The analyses were performed, as soon as possible, on the frozen samples. Seed added.

#1 It has been noted that the result for Dissolved Reactive Phosphorus was greater than that for Total Phosphorus, but within the analytical variation of these methods.

#2 It has been noted that the result for Dissolved Non-Purgeable Organic Carbon was greater than that for Non-Purgeable Organic Carbon, but within the analytical variation of these methods.

SUMMARY OF METHODS

The following table(s) gives a brief description of the methods used to conduct the analyses for this job. The detection limits given below are those attainable in a relatively clean matrix. Detection limits may be higher for individual samples should insufficient sample be available, or if the matrix requires that dilutions be performed during analysis.

Sample Type: Aqueous

Test	Method Description	Default Detection Limit	Sample No
Absorbance at 340, 440, 780nm	Filtered sample. Spectrophotometry, 1cm cell	0.002 AU cm^{-1}	1-4
Filtration, Unpreserved	Sample filtration through 0.45µm membrane filter.	-	1-4
Absorbance Filtration, 0.45 µm	Sample filtration through 0.45µm membrane filter for Absorbance.	-	1-4
Total Digestion	Nitric acid digestion. APHA 3030 E 22nd ed. 2012 (modified).	-	1-4
Total Kjeldahl Digestion - Trace level	Sulphuric acid digestion with copper sulphate catalyst.	-	1-4
Total Phosphorus Digestion	Acid persulphate digestion.	-	1-4
Total anions for anion/cation balance check	Calculation: sum of anions as mEquiv/L calculated from Alkalinity (bicarbonate), Chloride and Sulphate. Nitrate-N, Nitrite-N. Fluoride, Dissolved Reactive Phosphorus and Cyanide also included in calculation if available. APHA 1030 E 22nd ed. 2012.	0.07 meq/L	1-4
Total cations for anion/cation balance check	Sum of cations as mEquiv/L calculated from Sodium, Potassium, Calcium and Magnesium. Iron, Manganese, Aluminium, Zinc, Copper, Lithium, Total Ammoniacal-N and pH (H^+) also included in calculation if available. APHA 1030 E 22nd ed. 2012.	0.05 meq/L	1-4
Turbidity	Analysis using a Hach 2100N, Turbidity meter. APHA 2130 B 22nd ed. 2012.	0.05 NTU	1-4
pH	pH meter. APHA 4500-H^+ B 22nd ed. 2012. Note: It is not possible to achieve the APHA Maximum Storage Recommendation for this test (15 min) when samples are analysed upon receipt at the laboratory, and not in the field.	0.1 pH Units	1-4
Total Alkalinity	Titration to pH 4.5 (M-alkalinity), autotitrator. APHA 2320 B (Modified for alk <20) 22nd ed. 2012.	1.0 g/m^3 as $CaCO_3$	1-4
Bicarbonate	Calculation: from alkalinity and pH, valid where TDS is not >500 mg/L and alkalinity is almost entirely due to hydroxides, carbonates or bicarbonates. APHA 4500-CO_2 D 22nd ed. 2012.	1.0 g/m^3 at 25°C	1-4
Electrical Conductivity (EC)	Conductivity meter, 25°C. APHA 2510 B 22nd ed. 2012.	0.1 mS/m	1-4
Total Dissolved Solids (TDS)	Filtration through GF/C (1.2 µm), gravimetric. APHA 2540 C (modified; drying temperature of 103 - 105°C used rather than 180 ± 2°C) 22nd ed. 2012.	10 g/m^3	1-4
Filtration for dissolved metals analysis	Sample filtration through 0.45µm membrane filter and preservation with nitric acid. APHA 3030 B 22nd ed. 2012.	-	1-4
Total Arsenic	Nitric acid digestion, ICP-MS, trace level. APHA 3125 B 22nd ed. 2012 / US EPA 200.8.	0.0011 g/m^3	1-4
Boron	Analysed as received (after acid preservation, if required), ICP-MS, trace level. APHA 3125 B 22nd ed. 2012.	0.005 g/m^3	1-4
Dissolved Calcium	Filtered sample, ICP-MS, trace level. APHA 3125 B 22nd ed. 2012.	0.05 g/m^3	1-4
Lithium	Analysed as received (after acid preservation, if required), ICP-MS, trace level. APHA 3125 B 22nd ed. 2012.	0.0002 g/m^3	1-4
Dissolved Magnesium	Filtered sample, ICP-MS, trace level. APHA 3125 B 22nd ed. 2012.	0.02 g/m^3	1-4
Dissolved Potassium	Filtered sample, ICP-MS, trace level. APHA 3125 B 22nd ed. 2012.	0.05 g/m^3	1-4
Dissolved Sodium	Filtered sample, ICP-MS, trace level. APHA 3125 B 22nd ed. 2012.	0.02 g/m^3	1-4
Chloride	Filtered sample. Ferric thiocyanate colorimetry. Discrete Analyser. APHA 4500 Cl^- E (modified from continuous flow analysis) 22nd ed. 2012.	0.5 g/m^3	1-4

Sample Type: Aqueous			
Test	**Method Description**	**Default Detection Limit**	**Sample No**
Total Ammoniacal-N	Filtered sample. Phenol/hypochlorite colorimetry. Discrete Analyser. (NH_4-N = NH_4+-N + NH_3-N). APHA 4500-NH_3 F (modified from manual analysis) 22nd ed. 2012.	0.010 g/m^3	1-4
Nitrite-N	Automated Azo dye colorimetry, Flow injection analyser. APHA 4500-NO_3^- I 22nd ed. 2012 (modified).	0.002 g/m^3	1-4
Nitrate-N	Calculation: (Nitrate-N + Nitrite-N) - NO2N. In-House.	0.0010 g/m^3	1-4
Nitrate-N + Nitrite-N	Total oxidised nitrogen. Automated cadmium reduction, flow injection analyser. APHA 4500-NO_3^- I 22nd ed. 2012 (modified).	0.002 g/m^3	1-4
Total Kjeldahl Nitrogen (TKN)	Total Kjeldahl digestion, phenol/hypochlorite colorimetry (Discrete Analysis). Trace level. APHA 4500-Norg D. (modified) 4500 NH3 F (modified) 22nd ed. 2012.	0.05 g/m^3	1-4
Dissolved Reactive Phosphorus	Filtered sample. Molybdenum blue colorimetry. Discrete Analyser. APHA 4500-P E (modified from manual analysis) 22nd ed. 2012.	0.004 g/m^3	1-4
Total Phosphorus	Total phosphorus digestion, ascorbic acid colorimetry. Discrete Analyser. APHA 4500-P B & E (modified from manual analysis) 22nd ed. 2012. Also modified to include the use of a reductant to eliminate interference from arsenic present in the sample. NWASCA, Water & soil Miscellaneous Publication No. 38, 1982.	0.004 g/m^3	1-4
Reactive Silica	Filtered sample. Heteropoly blue colorimetry. Discrete analyser. APHA 4500-SiO_2 F (modified from flow injection analysis) 22nd ed. 2012.	0.10 g/m^3 as SiO_2	1-4
Sulphate	Filtered sample. Ion Chromatography. APHA 4110 B 22nd ed. 2012.	0.5 g/m^3	1-4
Total Biochemical Oxygen Demand ($TBOD_5$)	Incubation 5 days, DO meter, no nitrification inhibitor added, unseeded. Analysed at Hill Laboratories - Microbiology; 1 Clow Place, Hamilton. In-house.	0.4 g O_2/m^3	1-4
Dissolved Non-Purgeable Organic Carbon (DNPOC)	Acidification, purging to remove inorganic C, super-critical persulphate oxidation at 375°C, IR detection. APHA 5310 C (modified) 22nd ed. 2012.	0.3 g/m^3	1-4
Non-Purgeable Organic Carbon (NPOC)	Acidification, purging to remove inorganic C, super-critical persulphate oxidation at 375°C, IR detection. APHA 5310 C (modified) 22nd ed. 2012.	0.3 g/m^3	1-4
Chlorophyll a	Acetone extraction. Spectroscopy. APHA 10200 H (modified) 22nd ed. 2012.	0.003 g/m^3	1-4

These samples were collected by yourselves (or your agent) and analysed as received at the laboratory.

Samples are held at the laboratory after reporting for a length of time depending on the preservation used and the stability of the analytes being tested. Once the storage period is completed the samples are discarded unless otherwise advised by the client.

This report must not be reproduced, except in full, without the written consent of the signatory.

Graham Corban MSc Tech (Hons)
Client Services Manager - Environmental

Temperature and Dissolved Oxygen (DO)

Results were excellent for dissolved oxygen. All sites had saturated DO of >90%. Temperature was similar to dissolved oxygen which was excellent (<16°C) in the upper three sites. Temperature at lake Atiamuri was slightly higher however, within the satisfactory range of <20°C for the month of December.

Visual clarity

Visual clarity and turbidity are measures of the optical properties of water. Higher turbidity is associated with lower clarity and vice versa. The observed visual clarity at Tahunaatara catchment is somewhat similar to the turbidity observations. All sites had satisfactory (>1.6m and <4m) clarity measurement. None had excellent clarity (≥ 4m).

Turbidity

Results were excellent for all sites except Tahunaatara River which had a lower turbidity measurement however the level was satisfactory.

Biochemical Oxygen Demand (BOD)

Below detection levels at all sites which was excellent.

Ammonia

Not detected which is excellent.

Chlorophyll a

Excellent levels at all sites. Only detected at Atiamuri however the concentration is way below the standard of <0.02 g/m^3.

Total Nitrogen

Tahunaatara has a slightly poor nitrogen concentration with 0.73 g/m^3 recorded. The other three sites had satisfactory nitrogen concentrations of <0.5 g/m^3. Nitrogen at the catchment level appeared to be dominated by the nitrates. This record is consistent with the reported nitrogen concentrations in the Upland Waikato zone (Vant 2013).

Total Phosphorus

Satisfactory levels of phosphorus, both TP and DRP, were recorded at all four sites.

Arsenic

Not detected at Waikarakia and Pokaitu streams. However low concentrations were recorded at Tahunaatara and Lake Atiamuri. The upper Waikato River catchment which includes Tahunaatara have geothermal areas that contribute trace elements like arsenic to the freshwater system. So thermal activity is the likely cause of elevated arsenic concentration at the two sites.

Other results

Interestingly conductivity (a measure of dissolved ions/ salts in water) for Waikarakia, Pokaitu and Tahunaatara are low, in fact 50% lower than Lake Atiamuri. Major ion levels including elevated chloride concentration in the Waikato River is the likely cause of this. Atiamuri has twice as much major ion concentration and four times more chloride compared to the other three sites. In addition, reactive silica concentration decreases down the catchment.

Summary

Waikarakia stream has an overall excellent water quality. All indicators measured were within the expected levels. While the nitrogen level is considered satisfactory it is consistently elevated across the Tahunaatara catchment. The level of nitrogen at Waikarakia can be unusual in the local context given that the samples were taken close to the spring and the Upland zone is covered in native bush. However the results is insignificant when compared with similar sites across the upper Waikato region. Studies undertaken in the Taupo zone and monitoring data from sites in the Upland Waikato zone nearby have reported similar deterioration in nitrogen levels at streams that are spring-fed, with large underground aquifers (Vant 2013).

Pokaitu stream is somewhat similar to Waikarakia having excellent water quality. This is expected given the proximity of the two sites. Compared to Waikarakia stream the Pokaitu site has higher recreational value. A common swimming spot for the local community and adjacent to the local Kearoa Marae.

While the chemistry results is mixed: river water quality for ecological health across the Tahunaatara catchment is generally excellent. However in areas such as the Tahunaatara River where land use is more intensive, the observed water quality for ecological health is satisfactory. Water quality indicators for human uses such as recreation show excellent levels across the catchment.

All four sites sampled have been documented and records kept at the Waikato Regional Councils information management system for future reference if further sampling is required.

For any further clarification and/ or question please do not hesitate to contact the undersigned at Waikato Regional by email asaeli.tulagi@waikatoregion.govt.nz or phone DDI: 07 859 2736.

Yours sincerely,

Asaeli

Asaeli Tulagi |
Senior Environmental Scientist - Water Quality | Water Quality, Coast and Ecology |
Environmental Monitoring | Science and Strategy Directorate |
Waikato Regional Council | P: +64 7 859 2736 | F : +64 7 859 0998 | www.waikatoregion.govt.nz |

Private Bag 3038, Waikato Mail Centre, Hamilton 3240

6.3 Greenhouse Air Heating Calculations

Before running simulations in the MathCad, an Excel spreadsheet was used to compile weather data for all time periods. This data is shown below and comes from sources cited in the Methodology section.

Month	Day/Night	Temperature (Deg C)	Temperature (K)	Max Humidity at Cover	Humidity (%)	Cloud Cover (%)
Jan	Day	25	298		80	48
Jan	Night	17	290	0.013	80	48
Feb	Day	26	299		78	51
Feb	Night	17	290	0.013	78	51
Mar	Day	25	298		77	44
Mar	Night	16	289	0.012	77	44
Apr	Day	22	295		76	37
Apr	Night	13	286	0.01	76	37
May	Day	20	293		80	43
May	Night	13	286	0.01	80	43
Jun	Day	17	290		81	44
Jun	Night	10	283	0.009	81	44
Jul	Day	16	289		77	35
Jul	Night	9	282	0.008	77	35
Aug	Day	15	288		79	43
Aug	Night	8	281	0.008	79	43
Sep	Day	16	289		84	66
Sep	Night	10	283	0.009	84	66
Oct	Day	19	292		82	41
Oct	Night	11	284	0.009	82	41
Nov	Day	21	294		80	39
Nov	Night	12	285	0.009	80	39
Dec	Day	23	296		78	34
Dec	Night	14	287	0.011	78	34

Cloud Cover Factor	Tsky (K)	Incident Solar Radiation (W/m2)	Trasmissitivity	Absorbtivity
0.93	291	325	50.41	0.13
0.93	281			
0.91	292	325	0.71	0.13
0.91	281			
0.97	290	325	0.71	0.13
0.97	279			
1	285	326	0.71	0.13
1	274			
0.97	284	326	0.71	0.13
0.97	275			
0.98	280	326	0.71	0.13
0.98	272			
1	277	214	0.71	0.13
1	269			
0.97	278	214	0.71	0.13
0.97	269			
0.8	283	214	0.71	0.13
0.8	276			
0.98	282	578	0.71	0.13
0.98	272			
0.98	284	578	0.71	0.13
0.98	273			
1	286	578	0.71	0.13
1	275			

All information present for variables used in the MathCad program is shown below:

$H_E := 0.78$	Exterior relative humidity
$H_I := 0.75$	Interior relative humidity
$h_I := 7.4$	Interior convective heat transfer coefficient (W/m2*K)
$h_E := 9.1$	Exterior heat transfer coefficient (W/m2*K)
$\sigma := 5.67 \cdot 10^{-8}$	Stefan Boltzmann constant (W/m2/K4)
$A_{gl} := 205.2$	Area of cover (m2)
$\lambda := 2.5 \cdot 10^{6}$	Latent heat of condensation (J/kg)
$A_{gr} := 96$	Ground area (m2)
$k_c := 4.44 \cdot 10^{-4}$	Convective mass transfer coefficient (m/s)
$C_{am} := .015 \cdot H_I$	Mean absolute humidity at interior T (kg/m3)
$F := .9$	Radiative view factor between films
$C_a := .009 \cdot H_I$	Absolute humidity near cover (kg/m3)
$F_{ext} := 1.0$	Radiative view factor (exterior)
$F_{int} := 0.58$	Radiative view factor (interior)
$\rho_{air} := 1.225$	Density of air (kg/m3)
$V := 259.2$	Volume of greenhouse (m3)
$T := 3$	Air turnover rate (refill/h)
$M_{wi} := V \cdot \frac{T}{3600} \cdot H_E \cdot C_{am}$	Mass of water vapor entering greenhouse (kg/s)
$M_{ai} := \frac{(\rho_{air} \cdot V \cdot T)}{3600}$	Mass of air entering greenhoue (kg/s)
$M_i := \frac{(\rho_{air} \cdot V \cdot T)}{3600} + M_{wi}$	Mass of air and water entering greenhouse (kg/s)
$M_{wo} := \frac{V \cdot T}{3600} \cdot H_I \cdot C_{am}$	Mass of water vapor leaving greenhouse (kg/s)
$M_{ao} := \rho_{air} \cdot V \cdot \frac{T}{3600}$	Mass of air leaving greenhouse (kg/s)
$M_o := M_{ao} + M_{wo}$	Mass of air and water leaving greenhouse (kg/s)
$ET := 0.05$	Evapotranspiration rate (mm H20/h)
$M_{w3} := \frac{10^{6}(ET \cdot 2.45) \cdot A_{gr}}{\lambda \cdot 3600}$	Evapotranspiration rate (kg/s)
$C_{pa} := 1004$	Heat capacity of air (J/kg*K)

$C_{pw} := 1996$ Heat capacity of water vapor (J/kg*K)

$C_p := \frac{M_{wo}}{M_o}(C_{pw}) + \frac{M_{ao}}{M_o} \cdot C_{pa}$ Heat capacity of exiting air (J/kg*K)

$Q_g := 4.7$ Heat absorbed into water at 21 C (W/m^2)

$M_{w5} := k_c \cdot A_{gl} \cdot (C_{am} - C_a)$ Water removed by condensation on cover (kg/s)

$k_s := 0.10$ Conductivity of still air $\left(\frac{W}{m \cdot K}\right)$

$x := .025$ Distance between cover panes (m)

$CCF := 0.93$ Cloud cover factor

$I_{IH} := 0$ Incident radiation (W/m2)

$\alpha := 0.13$ Cover absorptivity

$\tau := 0.71$ Cover transmissiviy

$\rho := 0.16$ Cover reflectivity

Guess $t_{gl} := 280$ Temperature of inner cover pane (K)

$S_1 := 10$ Heat source input (W)

$M_{w4} := .005$ Water removed by dehumidifier (kg/s)

$t_{gl2} := 285$ Temperature of outer cover pane (K)

Key Temperatures $t_{sky} := 268$ Radiative sky temperature (K)

$t_E := 281$ Exterior Temperature (K)

$t_I := 290$ Interior temperature (K)

$t_{gr} := 281$ Ground temperature (K)

Given

$$S_1 + I_{IH} \cdot (\tau \cdot \tau) \cdot CCF \cdot A_{gl} + \left[\lambda \cdot (M_{w4} - M_{w3})\right] = h_I \cdot A_{gl} \cdot (t_I - t_{gl}) + \lambda \cdot k_c \cdot (C_{am} - C_a) \cdot A_{gl} + \sigma \cdot F \cdot \left(t_{gl}^4 - t_{gr}^4\right) \cdot A_{gr} + \left[M_o \cdot C_p \cdot (t_I - t_E) + Q_g \cdot A_{gr}\right]$$

$$M_{wi} + M_{w3} = M_{wo} + M_{w4} + M_{w5}$$

$$CCF \cdot A_{gl} \cdot I_{IH} \cdot \tau \cdot \alpha + h_I \cdot (t_I - t_{gl}) \cdot A_{gl} + \lambda k_c \cdot (C_{am} - C_a) \cdot A_{gl} + \sigma \cdot F_{int} \cdot \left(t_I^4 - t_{gl}^4\right) \cdot A_{gl} = \frac{k_s}{x} \cdot (t_{gl} - t_{gl2}) \cdot A_{gl} + \sigma \cdot F \cdot \left(t_{gl}^4 - t_{gl2}^4\right) \cdot A_{gl}$$

$$CCF \cdot A_{gl} \cdot I_{IH} \cdot \alpha + \left(\frac{k_s}{x}\right) \cdot (t_{gl} - t_{gl2}) \cdot A_{gl} + A_{gl} \cdot \sigma \cdot F \cdot \left(t_{gl}^4 - t_{gl2}^4\right) = h_E \cdot (t_{gl2} - t_E) \cdot A_{gl} + \sigma \cdot F_{ext} \cdot \left(t_{gl2}^4 - t_{sky}^4\right) \cdot A_{gl}$$

$$Find(S_1, t_{gl}, t_{gl2}, M_{w4}) = \begin{pmatrix} 1.323 \times 10^4 \\ 285.826 \\ 280.147 \\ 9.696 \times 10^{-4} \end{pmatrix}$$

Shown below are specifications for a possible heat pump to supply the specified heat:

OUTDOOR UNIT
S Series
PUMY-P YKM-A(-BS)

▸ Specifications

Model			PUMY-P112YKM-A (-BS)	PUMY-P125YKM-A (-BS)	PUMY-P140YKM-A (-BS)
Power source			3-phase 400V 50Hz	3-phase 400V 50Hz	3-phase 400V 50Hz
Cooling capacity	*1	kW	12.5	14.0	15.5
(Nominal)	*1	BTU / h	42,700	47,800	52,900
	Power input	kW	2.79	3.46	4.52
	Current input	A	4.24	5.26	6.87
	AEER/EER	kW / kW	4.07/4.48	3.71/4.05	3.19/3.43
Temp. range of	Indoor temp.	W.B.	15.0~24.0°C(59~75°F)	15.0~24.0°C(59~75°F)	15.0~24.0°C(59~75°F)
cooling	Outdoor temp.	D.B.	-5.0~46.0°C(23~115°F)	-5.0~46.0°C(23~115°F)	-5.0~46.0°C(23~115°F)
Heating capacity	*2	kW	14.0	16.0	18.0
(Nominal)	*2	BTU / h	47,800	54,600	61,400
	Power input	kW	3.13	3.74	4.47
	Current input	A	4.76	5.68	6.79
	ACOP/COP	kW / kW	4.14/4.47	3.99/4.28	3.78/4.03
Temp. range of	Indoor temp.	D.B.	15.0~27.0°C(59~81°F)	15.0~27.0°C(59~81°F)	15.0~27.0°C(59~81°F)
heating	Outdoor temp.	W.B.	-20.0°C(-4°F)	-20.0°C(-4°F)	-20.0°C(-4°F)
Indoor unit	Total capacity		50~130 % of outdoor unit capacity	50~130 % of outdoor unit capacity	50~130 % of outdoor unit capacity
connectable	Model / Quantity		P15~P140/9	P15~P140/10	P15~P140/12
Sound pressure level (measured in anechoic room)		dB <A>	49/51	50/52	51/54
Refrigerant piping	Liquid pipe	mm (in.)	9.52(3/8) Flare	9.52(3/8) Flare	9.52(3/8) Flare
diameter	Gas pipe	mm (in.)	15.88(5/8) Flare	15.88(5/8) Flare	15.88(5/8) Flare
FAN	Type x Quantity		Propeller Fan x 2	Propeller Fan x 2	Propeller Fan x 2
	Air flow rate	m³/min	110	110	120
		L/s	1,833	1,833	2,000
		cfm	3,884	3,884	4,237
	Motor output	kW	0.06 + 0.06	0.06 + 0.06	0.06 + 0.06
Compressor	Type x Quantity		Scroll hermetic compressor x 1	Scroll hermetic compressor x 1	Scroll hermetic compressor x 1
	Starting method		Inverter	Inverter	Inverter
	Motor output	kW	3.0	3.5	4.0
External finish			Galvanized Steel Sheet Munsell No. 3Y 7.8/1.1	Galvanized Steel Sheet Munsell No. 3Y 7.8/1.1	Galvanized Steel Sheet Munsell No. 3Y 7.8/1.1
External dimension HxWxD		mm	1,338 x 1,050 x 330 (+25)	1,338 x 1,050 x 330 (+25)	1,338 x 1,050 x 330 (+25)
		in.	52-11/16 x 41-11/32 x 13 (+1)	52-11/16 x 41-11/32 x 13 (+1)	52-11/16 x 41-11/32 x 13 (+1)
Protection	High pressure protection		High pressure Switch	High pressure Switch	High pressure Switch
devices	Inverter circuit (COMP./FAN)		Overcurrent detection, Overheat detection (Heatsink thermistor)	Overcurrent detection, Overheat detection (Heatsink thermistor)	Overcurrent detection, Overheat detection (Heatsink thermistor)
	Compressor		Compressor thermistor, Over current detection	Compressor thermistor, Over current detection	Compressor thermistor, Over current detection
	Fan motor		Overheating, Voltage protection	Overheating, Voltage protection	Overheating, Voltage protection
Refrigerant	Type x original charge		R410A 4.8kg	R410A 4.8kg	R410A 4.8kg
Net weight		kg (lbs)	125(276)	125(276)	125(276)
Heat exchanger			Plate fin coil	Plate fin coil	Plate fin coil
Defrosting method			Reversed refrigerant circuit	Reversed refrigerant circuit	Reversed refrigerant circuit
Optional parts			Joint: CMY-Y62-G-E Header: CMY-Y64/68-G-E	Joint: CMY-Y62-G-E Header: CMY-Y64/68-G-E	Joint: CMY-Y62-G-E Header: CMY-Y64/68-G-E

6.4 NKNT Sample Power Bill

Your next reading will be on or around 10 January 2017
Current charges

Meter 213575194	8 November 2016 to 7 December 2016 (30 days)				
Readings	Latest reading		Previous reading		Units
Register 1	13083 (Actual)	-	12718 (Actual)	=	365
Register 2	37827 (Actual)	-	36668 (Actual)	=	-1159
Charges	Units		Total electricity rate		Total
Fixed Energy Anytime	365	@	21.61c	=	$78.86
Export Seasonal	-1159	@	8.00c	=	-$92.72
Total				$	-13.86

Site charges	8 November 2016 to 7 December 2016 (30 days)				
Charges	Units		Total electricity rate		Total
Fixed Energy Daily	30	@	553.73c	=	$166.12
Electricity Authority Levy Charge	365	@	0.19c	=	$0.69
Total				$	166.81

Electricity you've used – in kilowatt hours (kWh)

NOTE – This bar graph shows your approximate monthly consumption. It's worked out based on your average daily consumption, then calculated for a calendar month.

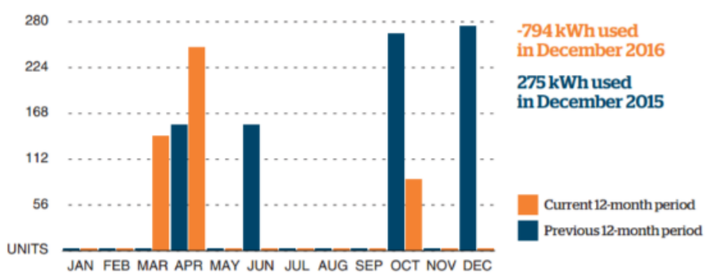

Total amount for all meters **$152.95**